
DR SHUTAO HE (Orcid ID : 0000-0002-9023-5123)

DR XIAOFENG BIAN (Orcid ID : 0000-0001-7660-9160)

DR LING YUAN (Orcid ID : 0000-0003-4767-5761)

Article type : Original Article

Dynamic network biomarker analysis discovers IbNAC083 in initiation and regulation of sweet potato root tuberization

Shutao He^{1,#}, Hongxia Wang^{2,#}, Xiaomeng Hao^{2,3,#}, Yinliang Wu^{2,3}, Xiaofeng Bian², Minhao Yin^{2,4}, Yandi Zhang^{2,3}, Weijuan Fan², Hao Dai¹, Ling Yuan⁵, Peng Zhang^{2,3,*}, Luonan Chen^{1,6,7*}

¹ State Key Laboratory of Cell Biology, Shanghai Institute of Biochemistry and Cell Biology, CAS Center for Excellence in Molecular Cell Science, Chinese Academy of Sciences, Shanghai 200031, China

² National Key Laboratory of Plant Molecular Genetics, CAS Center for Excellence in Molecular Plant Sciences, Institute of Plant Physiology and Ecology, Chinese Academy of Sciences, Shanghai 200032, China

³ University of Chinese Academy of Sciences, Beijing 100049, China

⁴ Henan University of Science and Technology, Luoyang 471000, China

⁵ University of Kentucky, Lexington 40506, USA

This article has been accepted for publication and undergone full peer review but has not been through the copyediting, typesetting, pagination and proofreading process, which may lead to differences between this version and the [Version of Record](#). Please cite this article as [doi: 10.1111/TPJ.15478](https://doi.org/10.1111/TPJ.15478)

This article is protected by copyright. All rights reserved

⁶ Key Laboratory of Systems Health Science of Zhejiang Province, Hangzhou Institute for Advanced Study, University of Chinese Academy of Sciences, Chinese Academy of Sciences, Hangzhou 310024, China

⁷ School of Life Science and Technology, ShanghaiTech University, Shanghai 201210, China

RUNNING TITLE

DNB analysis of storage root development in sweet potato

Keywords: sweet potato; storage root development; transcriptome dynamics; coexpression network; dynamic network biomarker; tipping point; IbNAC083

*** Corresponding authors:**

Luonan Chen (luchen@sibcb.ac.cn, ORCID:0000-0002-3960-0068) or Peng Zhang (zhangpeng@cemps.ac.cn, ORCID: 0000-0002-4868-1306)

#These authors contributed equally to this work.

SUMMARY

The initiation and development of storage roots are intricately regulated by a transcriptional regulatory network. One key challenge is to accurately pinpoint the tipping point during the transition from pre-swelling to storage roots and to identify the core regulators governing such a critical transition. To solve this problem, we performed a dynamic network biomarker (DNB) analysis of transcriptomic dynamics during sweet potato root development. Firstly, our analysis identified stage-specific expression patterns for a significant proportion (>9%) of the sweet potato genes and unraveled the chronology of events that happen at the early and later stages of root development. Then, the results showed that different root developmental stages can be depicted by coexpressed modules of sweet potato genes. Moreover, we identified key components as well as their transcriptional regulatory network determining root development. Furthermore, through DNB analysis, an early-stage with root diameter 3.5 mm was identified as the critical period of storage root swelling initiation, which is consistent with morphological and metabolic changes. In particular, we identified a NAC-domain transcription factor, IbNAC083, as a core regulator of this initiation in the DNB-associated network. Further analyses and experiments showed that IbNAC083, along with its associated differentially expressed genes, induced dysfunction of metabolism processes, including biosynthesis of lignin, flavonol and starch, thus leading to the transition to swelling roots.

INTRODUCTION

Sweet potato (*Ipomoea batatas* L.) is the sixth largest food crop in the world. The widely grown crop is high in nutrient content and suitable for multiple food and industrial uses (Dong et al., 2019). Storage root, the carbohydrate storage organ that is also used for vegetative propagation, is the most economically important part of sweet potato, as well as an excellent model for studying organogenesis and evolution. Therefore, much of research is focusing on the mechanisms underlying storage root formation and development.

The initiation and development of storage roots are complicated biological processes influenced by both internal and external factors. Storage roots (SR) of sweet potato are specialized roots that

develop from adventitious roots at the anatomical level (Wilson and Lowe, 1973). In sweet potato, roots are classified into young roots, non-tuberous roots, pencil-like and tuberous roots according to degree of stele lignification and primary cambium activity (Togari, 1950). Firstly, the developmental process begins by the genesis of vascular cambiums from procambial cells between the primary phloem and primary xylem of young fibrous roots, resulting into the formation of circular primary cambium (Ravi et al., 2009). Afterward, secondary meristems, including the meristems around vessels and anomalous secondary cambiums, differentiate into the xylem. Furthermore, cell divisions and expansions proceed in the primary cambium and secondary meristems, accompanying with the divisions of parenchyma cells in the xylem, resulting into the root expansion. During this expansion phase, the parenchyma cells accumulate a mass of photosynthates, specifically starch (Firon et al., 2013). Pencil roots do not undergo into SR by the process of lignification (Villordon et al., 2009), indicating that stele lignification at the early root developmental stage influences SR development process (Togari, 1950). To facilitate the study of sweet potato root development, 20 stages (S1 to S20) have been classified according to the root diameters (Wang et al., 2016). Further, transcriptomics study validated the down-regulation of lignin biosynthesis and up-regulation of starch biosynthesis genes at early stage of SR formation (Firon et al., 2013). The formation and development of storage roots strongly correlate to the levels of endogenous phytohormones. Storage root swelling is the consequence of the synergistic interaction of several phytohormones, including cytokinins (CTKs), abscisic acid (ABA), auxin (IAA), jasmonic acid (JA), and gibberellin (GAs) (Ravi et al., 2009, Tanaka et al., 2008, Nakatani, 1994, Spence and Humphries, 1972, Nakatani and Komeichi, 1991, Noh et al., 2010, Singh et al., 2019).

Recently, considerable progresses about the isolation and characterization of genes related to storage root formation have been made, which can be grouped into four categories: (1) Cell division-related genes, such as *Cyclin A-like* and *Cyclin D-like* that are the key cell division-regulator genes (Firon et al., 2013); (2) Expansion-related genes, including *IbEXP1* that affects the weight and number of storage roots (Noh et al., 2013); (3) Lignin biosynthesis-related genes, since lignification of the stele restrains the transition of adventitious roots to storage roots (Belehu et al., 2004); (4) Transcription factor genes, such as *IbMADS* that affects the enlargement of the storage roots (Ku et al., 2008), *SRD1* that is essential for the initiation and development of tuberous roots by influencing auxin synthesis (Noh

et al., 2010), as well as KNOXI homeobox and NAC homeobox genes that affect storage roots development with affecting lignin content (Firon et al., 2013, Tanaka et al., 2008). Specification into distinctive xylem cells affecting lignin content can be affected by various NAM/ATAF/CUC (NAC) domain transcription factors such as XND1, VND and AtNAC083 in Arabidopsis (Yamaguchi et al., 2011). AtNAC083 interacts with VND proteins and other NAC domain proteins, which regulates xylem cell differentiation, implying the significance of a transcriptional network regulating xylem specification (Yamaguchi et al., 2010).

Currently, the transcriptional mechanisms mediating initiation and progression of root swelling, a nonlinear transitional process, remain unclear. In other words, how the swelling process is initiated and what is the critical state (tipping point) with its core regulators during root swelling development are largely unknown. Transcriptomic analysis is an effective approach to study transcriptional mechanisms, which gives an overview of spatiotemporal gene expression profiles and associates biological functions with co-expressed genes (Silva et al., 2016, Vesty et al., 2016). Dynamical study of transcriptome data thus gives us a powerful tool to explore the mechanism underlying phase transition of developing roots in a genome-wide scale (Chen, 2016). However, the majority of the traditional studies concentrate on static molecular biomarkers, which mainly distinguish different development states of storage root due to their static features, e.g., via using 'differential expressions of molecules' (Dong et al., 2019, Wang et al., 2015, Firon et al., 2013). In other words, it is difficult to determine the critical state or catch dynamical signals occurring at the tipping-point, which is a key to reveal the critical transition with its core regulators from fibrous roots to storage roots. Recently, dynamic network biomarker (DNB) method, which is a model-free method, has been developed to recognize early signal of a critical transition as well as its core regulators in many biological problems, involving hepatocellular carcinoma and type-2 diabetes, based on the omics data and nonlinear dynamical theory (Chen et al., 2012, Li et al., 2017, Li et al., 2014, Liu, 2013, Yang et al., 2018, Zhang et al., 2019, Jiang et al., 2020). Whereas DNB has been successfully used in medical research, its application in plant research remains scarce (Zhang et al., 2019). Nevertheless, DNB is an ideal method to identify the tipping-point or pre-swelling state (just before the dramatical transition to the swelling state) during storage root developmental process, based on 'differential associations among molecules' (or differential networks) in a dynamical

manner, and further determine the corresponding core regulators or regulatory network, in contrast to the traditional strategy 'differential expressions of molecules' (or differential molecules/genes).

Here, based on our gene expression profiles of sweet potato roots at different developmental stages, we studied the molecular mechanisms of storage roots development from the perspectives of dynamics and network, and identified the tipping point of storage root swelling process by DNB method. In particular, we discovered that IbNAC083, a member of the DNB-associated network, not only regulates sweet potato storage roots initiation but also quantifies the tipping point of this process, which was validated by biological experimental analysis. Collectively, our study not only identified the core regulator and its associated DNB network which tightly regulates the critical developmental transition during root swelling process, but also provides an information-rich resource for investigating the functions of key components in storage root development.

RESULTS

Characterizing root phenotypes at different developmental stages of sweet potato roots for RNA-Seq analysis

Several important physiological parameters were analyzed in roots at seven developmental stages (S4-20) representing major events occurring within the root, including the early fibrous and pencil root development, and the later storage root formation and swelling (Figure 1a). The initial swelling roots showed circular primary cambia (S10 and S12), and the storage roots at later stages displayed secondary cambia and anomalous meristems (S16), which had more parenchyma cells (Figure 1b). Toluidine blue staining for lignin revealed a continuously decreased number of lignified cells surrounding xylem bundles and increased starch granules from fibrous roots (S4) to storage roots (S16). To verify this result, the lignin and starch levels of roots at different developmental stages were measured. The lignin content decreased gradually from S8 (average of 73.6%) to S20 (average of 16.6%), whereas the starch content increased progressively from S8 (average of 1.9%) to S20 (average of 68.9%) (Figure 1c, d). In addition, sucrose content increased from S4 and reached plateau at S12 to S16 before a decrease. The levels of glucose and fructose remained low prior to S14, followed by a sharp increase at S16 before a decrease. Maltose level was barely detectable until S16,

followed by a sharp increase (Figure 1e).

To decipher the molecular mechanism underlying the initiation and development of sweet potato storage roots, we conducted RNA-Seq analysis using total RNA extracted from roots at seven developmental stages. After removing of adaptors and reads containing low-quality nucleotides, more than 47 million clean reads (average ~56 million reads) were obtained for each sample (Table S1) and aligned to the sweet potato genome with the size of 466 Mb using TopHat. More than 77% of the clean reads were aligned to the genome, and more than 72% of the clean reads were unique mapped reads (Table S1). The mapped files were processed via StringTie (v1.3.3b), which generated a transcriptome assembly with a total of 99697 gene loci, including 75502 annotated and 24195 novel gene loci (Table S2). The uniquely mapped reads for each sample were processed via RSEM (v1.3.1) to obtain the normalized expression level as transcripts per million reads (TPM) for all the sweet potato genes. Overall, a total of ~77% genes (TPM > 0.1) were identified as expressed in at least one of the 7 stages (Table S3), and the number of expressed genes in different stage samples varied from 56.4% (S4) to 65.2% (S14).

Global transcriptome analysis of sweet potato roots at different developmental stages

To study the global differences of the transcriptome dynamics during root development of sweet potato, we performed PCA, GO analysis, and unsupervised hierarchical clustering based on the TPM values for all the expressed genes in at least one of the 7 developmental stages. PCA revealed that sweet potato root transcriptomes were clustered into four groups, (i) fibrous roots (S4 and S8), (ii) early stages of storage root development (S10 and S12), (iii) middle stages of storage root development (S14 and S16), and (iv) mature stage of storage root development (S20) (Figure 2a), which reflects the progression from fibrous roots to mature storage roots (Figure 1a). To explore the biological functions that distinguish these samples in different developmental stages, we selected the 500 genes with the largest load and the 500 genes with the smallest load in principal component 1 (PC1) and principal component 2 (PC2) and performed GO enrichment analysis. As shown in Figure 2b, the biological functions with most significant changes during the development of sweet potato roots included carbohydrate metabolic process, cell wall, transcription regulator activity, protein metabolic process, secondary metabolic process and response to stress, which were in agreement with previous studies

(Firon et al., 2013). Furthermore, the hierarchical clustering analysis (Figure 2c) showed that all samples were clustered into four independent groups, consistent with the clustering by PCA (Figure 2a). Clearly, only samples in S10 stage were dispersed in both fibrous roots state and early developmental state, indicating that they might be at the critical stage before the swelling transition to storage roots.

Preferentially expressed genes in each root developmental stage of sweet potato

We analyzed the genes expressed at a particular stage of root development by using the stage specificity (SS) algorithm (Zhan et al., 2015) with SS score > 0.5. According to this criterion, we characterized a total of 6791 genes particularly expressed at a special root developmental stage (Table S4). Collectively, 196 TFs belonging to 28 gene families displayed developmental stage-specific expression profile. The members of several TF families, including HB, MYB, bHLH and HSF TF families, showed high representation. Figure S1a depicts the stage-specific gene expression patterns during sweet potato root development. The variable number and proportion of preferentially/specifically expressed genes suggest that each stage has its own independent developmental programs.

The GO enrichment analysis of all the stage-specific genes showed representation of genes associated with reproductive processes, cell wall organization, carbohydrate metabolic processes, and response to stress/hormone. These processes are related to various aspects of root development. In general, the fibrous root stages (S4 and S8) were marked by functions related to inorganic anion transport, primary metabolic process, and response to stimulus (Figure S1b). The early stages (S10 and S12) were marked by functions associated with brassinosteroid biosynthetic process and hormone biosynthetic process. Interestingly, there were no significantly enriched GO terms at S10 stage, indicating that S10 without significant highly expressed biological functions might be in the critical period of storage root swelling transition or a pre-swelling state, which is in line with the conclusion of hierarchical clustering result (Figure 2c). During the middle stages (S14 and S16), biological processes related to cell wall reorganization, carbohydrate metabolic process, hormone metabolic regulation, and regulation of transcription were overrepresented. At the mature stage (S20), GO terms related to starch biosynthesis process, abscisic acid metabolism, and cell wall were overrepresented. In conclusion, a

set of genes, containing those encoding TFs, implement stage-specific functions during root developmental process in sweet potato, potentially providing hints to the transition stage of tuberous root swelling.

We performed RT-qPCR analysis for 17 genes displaying stage-specific expression. The results revealed that the expression patterns and stage-specific expression of the tested genes resembled those obtained by RNA-Seq (Figure S2), implying the accuracy of RNA-Seq data. For the majority of the genes tested, the correlation coefficient was ≥ 0.70 between the RNA-Seq and RT-qPCR analysis (Figure S2).

Characterizing transcriptional reprogramming during sweet potato root development

DESeq2 identified 13063 differentially expressed genes (DEGs), and DEGs were obtained at each stage of root development as compared with the previous adjacent stage (Table S5). Wherein, 7 genes were found as DEGs uniquely at S8 stage compared with S4 stage; 3175 genes were identified as DEGs specially at S10 stage compared with S8 stage; 609 genes were found as DEGs specially at S12 stage compared with S10 stage; 2412 genes were found as DEGs uniquely at S14 stage compared with S12 stage; 336 genes were identified as DEGs uniquely at S16 stage compared with S14 stage; and 3044 genes were identified as DEGs specially at S20 stage compared with S16 stage. There were 3480 genes differentially expressed at more than one stage. Many of these DEGs have not been previously described as related to root development. Previous study has analyzed the genome-wide transcriptional profiling of sweet potato root at seven different developmental stages using a customized microarray including 39724 genes (Wang et al., 2015). Based on the root diameter, we matched our samples with the samples at the same developmental stage in the previous study. All DEGs identified in the microarray analysis in an earlier study (Wang et al., 2015) were also differentially expressed in our study, but only accounted for approximately 17.8% of DEGs in our dataset (Figure 3a, and larger image in Figure S3), indicating that our dataset captures a larger proportion of root developmental transcriptional changes and can be used to model biologically relevant gene expression changes during root development.

Next, the genes were separated into sets of up-regulated and down-regulated DEGs and were sorted

based on the time at which they were first differentially expressed. Several biological processes particularly enriched at various stages of root development were identified by the GO enrichment analysis of these gene sets (Figure 3b). The analysis showed that a massive onset of down-regulation enriched biological processes preceded that of up-regulation, and various waves of coordinated biological functions of gene expression changes can be identified during root development. Various metabolic processes related GO terms, such as cellular amino acid and derivative metabolic process, lipid metabolic process, and secondary metabolic process, were significantly repressed, particularly at S10 stage compared with S8 stage. Likewise, compared with S8 stage, regulation-related GO terms, including transcription factor activity, transcription regulator activity, protein modification process, and kinase activity, were highly enriched at S10 stage in the down-regulated genes. Additionally, development-related genes, involving in post-embryonic development and multicellular organismal development, exhibited transcriptional activation during the middle developmental stages (S14 and S16). Interestingly, we observed significant activation of genes are related to GO terms of cell wall and carbohydrate metabolic process at S14 stage, followed by repression at S16 stage, suggesting higher activities of cell wall metabolism and starch accumulation during middle stages of root swelling progression. Thereafter, the genes associated with carbohydrate metabolism were observed to be more active at S20 stage.

Characterizing gene regulatory network rewiring during sweet potato root development

The chronology of transcriptional states during root development was discerned by mining our RNA-Seq data. First, DEGs at each developmental stage were divided into two gene sets, i.e., up-regulated and down-regulated DEGs. Then, according to their predicted function as transcriptional regulators (termed regulator genes) or as having a different function (termed regulated genes), we divided these genes into two additional sets. In order to investigate the biological significances and regulatory directionality of each gene set (termed transcriptional state), the gene sets of the 20 transcriptional states were analyzed for enrichment of functional categories and promoter motifs (Figure 3c). The first wave of transcriptional changes is characterized by genes related to transcriptional regulation, including AP2/ERFs, bZIPs and MYBs, and other genes associated with metabolism and development, and begins at the transition from S8 to S10 stage. These regulatory

genes might be crucial to the regulation of other regulator genes and regulated genes appear in the contemporaneous or subsequent developmental stage transitions, which are linked to root developmental processes, such as cell differentiation, signal transduction, organ development, cell wall and carbohydrate metabolism. For instance, in the DEGs of state 9, DNA motif that can be bound by AP2/ERFs which was transcribed in previous states 2, 3, 6, 7 and contemporaneous states 10 and 11, are enriched. In state 9, genes involved in stress response, cell wall and metabolism process are enriched, which is consistent with previous studies showing that AP2/ERF genes play various roles in the regulation of several developmental processes, such as floral organ development and leaf epidermal cell development, and response to multiple forms of biotic and abiotic stress (Riechmann and Meyerowitz, 1998).

Further, to predict directional interactions between the regulator genes and the regulated genes related to the various transcriptional states, a gene regulatory network was established using the TF DNA-binding motif information. As shown in Figure 3d, when a specific DNA-binding motif is enriched in one transcriptional state, that state (indicated by a square node) is linked to the corresponding differentially expressed TF genes (indicated by a circular node and sorted based on the time at which they were first differentially expressed). In the network, TFs were likely to regulate transcriptional levels of genes at either single or several transcriptional states. Particularly, due to TFs that become active in the states (state 1 and state 4) showing the first wave of transcriptional activity might be crucial to the regulation of subsequent transcriptional activity, the regulatory relationships between TFs assigned to these states were predicted using the network. State 1 and State 4 contain the TFs IbWRKY75, IbMYB61, IbMYB30, IbHY5, IbHSFA6B, IbEIN3, IbERF109, and IbABF2, which are the most active TFs because of the overrepresentation of their DNA binding motifs in the promoters of genes assigned to the majority of the differential expression transcriptional states. This prediction is consistent with previous reports indicating that these TFs are modulators of root development (Devaiah et al., 2007, Romano et al., 2012, Sakaoka et al., 2018, Van Gelderen et al., 2018, Huang et al., 2016, Li et al., 2020a, Cai et al., 2014, Garcia et al., 2014). Furthermore, other stages contain the TFs IbWOX8, IbTGA3, IbRAP2, IbPHL2, IbATHB3, IbMYB08, IbKN1, IbARF8, IbANT, and IbAGL42, of which corresponding mutants show altered root development (Petricka et al., 2012, Farinati et al., 2010,

Eysholdt-Derzso and Sauter, 2017, Bonke et al., 2003, Bomal et al., 2008, Woerlen et al., 2017, Gutierrez et al., 2009, Randall et al., 2015, Hacham et al., 2011, Silva et al., 2016). Moreover, *IbKNOX1* genes have been shown to regulate cytokinin levels, thus affecting sweet potato storage root development (Tanaka et al., 2008, Ravi et al., 2009).

Analysis of transcriptional modules associated with root development of sweet potato

Weighted gene coexpression network analysis (WGCNA) was used to identify coexpressed genes. Through this gene regulatory network (GRN) analysis, several major subnetworks were formed, which are characterized by interaction relationships among genes showing similar expression patterns, termed coexpression modules. Fifteen modules (containing 33-3743 genes) were identified (Figure 4a and Table S6). We associated each coexpression module with root developmental stages and physiological phenotypes using Pearson correlation coefficient analysis. Twelve coexpression modules showed significant correlation ($r \geq 0.50$ and $P\text{-value} \leq 0.01$) with root developmental stages. Most of the modules were associated with a particular root development stage only; however, a few of them were correlated with more than one root development stage, such as the black and blue modules in Figure 4b.

The S10 stage seems to be a critical period for the swelling of sweet potato roots (Figure 2c, Figure 3b-d and Figure S1b). Considering that modules associated with S10 stage might be responsible for the swelling in root development program, we examined the GRNs that connect the TFs with corresponding coexpressed target genes harboring remarkably overrepresented TF binding motifs at S10 and its adjacent developmental periods (S8 and S12) (Figure 4b-c). Coexpressed genes involved in the modules related to S8, S10 and S12 were used to perform this analysis and we found coexpressed modules associating the overrepresented TF binding motifs with the known TFs and specific GO categories that are remarkably enriched in their target genes. The transcriptional modules in S8 (black, salmon and blue modules) included TFs with significantly enriched motifs, like *IbNAC083*, *IbERF109*, *IbWRKY53*, *IbMYB30* and *IbBEH4*, and target genes related to GO categories of regulation of cell wall reorganization and response to hormone stimulus (Figure 4b). At S10 (tan and red modules), motifs associated with TFs like *IbWOX8*, *IbPHL2*, *IbERF10*, *IbWRKY48*, and *IbKN1* were

enriched (Figure 4c), and their associated target genes are involved in cellulose biosynthetic process, cellular cell wall organization or biogenesis, chromatin silencing by small RNA and primary metabolism. Similarly, motifs associated with TFs, such as IbMYB08, IbNAC092, IbWRKY65, IbTCP15 and IbBH130, and target genes involved in secondary metabolic process, hormone transport, gibberellin and salicylic acid metabolism, oxidation reduction and carbohydrate transport, were enriched in the transcriptional modules at S12 stage (Figure 4d). Several these regulatory motifs and TFs are related to root development and play vital roles coordinately in gene transcriptional activation. For instance, some reported TFs associated with root development overrepresented in the differential expression regulatory network (Figure 3d), such as IbERF109, IbMYB30, IbMYB61, IbHSFA6B, IbPHL2, IbWOX8, IbANT, IbKN1 and IbMYB08, were also enriched in the modules associated with S8, S10 and S12 stages. Moreover, IbWRKY53 also plays a crucial role in root elongation (Li et al., 2020b). Overall, some key transcriptional modules were characterized as important modulators and their roles in regulating root development and decision of root phenotype were revealed.

IbNAC083 was identified as one core regulator of DNB members and played a key role in storage root initiation

To precisely identify the tipping point of root swelling initiation, the phase transition model based on DNB method was used. According to the nonlinear dynamic theory, the tipping point is the critical state just before the transition, and its DNB accords with a unique gene expression profile characterized by collective fluctuation and strong correlation. Previous studies (Chen et al., 2012, Liu et al., 2014, Liu et al., 2015) have shown that, at the critical state, (i) the transcriptional level of a group of DNB genes becomes highly fluctuated, indicated by coefficient of variance, CV_{in} ; (ii) the transcriptional level of the DNB genes exhibits high correlation, represented by the absolute PCC values, PCC_{in} ; and (iii) associations between DNB genes and other genes significantly decrease, represented by the absolute PCC values (PCC_{out}). Considering all the above criteria, we used an index (CI) as the comprehensive signal of DNB method. When CI comes up to the peak or rises dramatically during the measured stages, the corresponding stage is the critical state of the biological system. As shown in Figure 5a, S10 stage is the tipping point because of the highest CI score. This result was in line with the morphological changes of sweet potato roots (Figure 1a, b) and the dynamics of gene expression

(Figure 2c, Figure S1b, and Figure 3b, c). We identified 86 genes dedicating to the *CI* score as the DNB members. Some of these DNB genes play important roles in root development. For instance, reduction in root growth was observed in MGD mutants under Pi-starvation (Kobayashi et al., 2009). In Arabidopsis, NAP1-RELATED PROTEIN1/2 (NRP1/2) that is a H2A/H2B histone chaperone, is essential to maintain root stem cell niche (Ma et al., 2018). In rice, *VILLIN2* (*VLN2*) mutant seedling shows malformed organs, such as twisted roots and shoots (Wu et al., 2015). Additionally, DNB members including EDS1, RPS13, ELP2, RPL3 and CUL1 also play key roles in root growth and development (Kim et al., 2012, Ito et al., 2000, Jia et al., 2015, Popescu and Tumer, 2004, Woodward et al., 2007).

To explore the key regulators for root swelling initiation, we predicted interactions between TF genes and DNB genes based on the TF binding motif information and the expression correlation (absolute Pearson correlation coefficient $|PCC| > 0.8$). We then ranked the DNB-regulating TFs according to the criteria of importance in regulatory network of DNB members, differential patterns, dynamic regulatory patterns of DEGs, transcriptional regulatory patterns of coexpressed module (see Ranking scheme for regulators of DNB members in Experimental procedures). Through this analysis, there were 5 TFs (IbNAC083, IbHFA6B.1, IbMYB61.1, IbERF109.1 and IbBEH4.1) that meet these screening criteria, i.e., belonging to DEGs of S8-S12, enriched motifs associated TFs regulating DEGs during S8-S10 and enriched motifs associated TFs in the S8 module. Based on the ratio of DEGs in a DNB set regulated by each TF (IbNAC083: 67%; IbHFA6B.1: 50%; IbMYB61.1: 50%; IbERF109.1: 40%; IbBEH4.1: 33%), IbNAC083 was selected as the top candidate for further functional study due to its highest ratio.

To determine the molecular function of IbNAC083 in storage root development, the expression profile and the cellular localization of IbNAC083 were examined. *IbNAC083* was expressed in various root cell types, especially in the stele, and localized in the nucleus (Figure S4a-c). To further explore the function of IbNAC083 in storage root initiation, transgenic sweet potato plants showing down-regulated *IbNAC083* expression by RNAi were generated. Compared to the wild type (WT), the expression levels of *IbNAC083* in four independent transgenic lines were decreased significantly (Figure 5b). Five-month-old transgenic and WT plants were collected from the field, *IbNAC083*-RNAi transgenic

plants showed decreased storage root size and more pencil roots compared to WT (Figure 5c). The root biomass per plant varied from 0.35 kg to 2.11 kg for the transgenic lines (Figure 5d), which was considerably less than the average fresh weight of WT (2.86 kg). The average pencil root number per plant was 6.33 in WT, but ranged from 8.73 to 13.2 for the transgenic lines (Figure 5e). The average storage root number per plant ranged from 0.40 to 2.11 for the transgenic lines (Figure 5f), which was dramatically less than the number for WT (3.67). These results suggested that IbNAC083 affects the root swelling initiation and promotes storage root formation.

Rewiring of IbNAC083-subnetwork before and after the tipping point

Storage root development is an intricate and dynamic process, including various genes working synergistically (Wang et al., 2015, Firon et al., 2013, Dong et al., 2019). DNB genes positioned in upstream of pathways are important for the initiation and development of complex biological progression (Chen et al., 2012, Li et al., 2014, Li et al., 2017). Thus, IbNAC083-related regulations (or network rewiring) were analyzed to systematically investigate the function of IbNAC083 in storage root swelling at a network level. Based on the well-known molecular interactions of plant biology in the STRING database, IbNAC083 and its 78 neighboring genes were integrated into IbNAC083-centered network and the nodes of this network were weighted based on the Z-score converted data of their real transcriptional expressions throughout the three developmental stages (S8, S10 and S12) (Figure 6a and Table S7). The expression levels of 63 neighboring genes (80% of all IbNAC083 neighboring genes) are switching, from high (low) to low (high) levels before and after the critical stage of storage root initiation (S10 stage). This result suggested that IbNAC083 has a significant influence on storage root swelling initiation, directly or proximally affecting these DEGs with switching expression patterns at a molecular network level.

IbNAC083 is located upstream of root swelling initiation associated processes

Further, we examined the association between the initiation of storage root swelling and biological functions overrepresented by IbNAC083 and 63 inversely expressed DEGs before and after the tipping point of storage root swelling (Figure 6b). The enriched functions were related primarily to regulation of gene expression and metabolic processes (e.g., lignin and flavonol biosynthesis). These enriched

biological processes affect storage root development by association with signals in cell growth and division (Firon et al., 2013, Belehu et al., 2004) and auxin transport (Brown et al., 2001, Peer et al., 2013, Tan et al., 2019). The dynamic phenotypes of *IbNAC083* and its inversely expressed DEGs implied the complication and time-dependence of dysfunctions in swelling-associated processes during the initiation of storage root swelling (Figure 6a, b). The majority of the biological processes were related to regulation of metabolism (e.g., macromolecule metabolism and flavonol biosynthesis) and oxidation reduction were dysregulated before the critical state, whereas the typical storage root formation mechanism (i.e., organ development) was dysregulated after the critical stage. Dysfunction in lignin biosynthetic process, peculiarly those including *IbNAC083*, happened across the root swelling initiation stage.

To further investigate how *IbNAC083* affects the initiation of root swelling, we performed RNA-Seq analysis of the initial swelling roots of WT (S12-S14) and *IbNAC083*-RNAi transgenic plants (S12-S14) grown in the field (Table S8 and Table S9). Compared with WT, 5443 DEGs (adjusted *P*-value < 0.05) were identified in the roots of transgenic plants. GO enrichment (Figure 6c) showed that the biological processes associated with the DEGs close resemble those observed in the network analysis (Figure 6b). *IbNAC083*-RNAi resulted in significant changes in GO terms related to metabolic processes, including lignin and starch metabolism, which was supported by significant changes of lignin and starch content (Figure S5a, b). RT-qPCR analysis confirmed the significant changes of expression of many key genes related to lignin metabolism (*IbC4H*, *IbCAD*, *IbCCR*, *IbCOMT* and *IbCCoAOMT*) and starch metabolism (*IbAGPa*, *IbAGPb*, *IbGBSSI*, *IbSBEI*, *IbSBEII*, *IbSS*, *Ib α -amylase* and *Ib β -amylase*) in the transgenic plants (Figure S5c, d).

According to the above analyses, the dynamic changes of biological processes resulted proximally from the function or dysregulation in *IbNAC083* during the swelling initiation of storage root. Next, whether *IbNAC083* could regulate well-known genes associated with root development in a cascade was identified. We examined 66 root development related genes, e.g., those related to cell cycle, cell wall biogenesis and histone phosphorylation. The expression of 30 genes was affected by *IbNAC083*, which were also found in our root developmental series transcriptomic data (Figure 6d). 16 genes of

them are DEGs identified in the developmental transcriptomic analysis (Figure 6d). Seven genes co-expressed with *IbNAC083*, of which three were positively correlated with *IbNAC083* expression, and the rest were negatively correlated to *IbNAC083* (Figure 6d). These results suggested that *IbNAC083* could affect the expression of genes related to root development in a cascade manner, which might be significant to initiation of sweet potato storage roots.

DISCUSSION

The molecular mechanisms underlying sweet potato root development are still poorly understood. Initiation of storage root swelling is the critical stage that determines crop yield. It is difficult to elucidate the regulatory mechanism that determines the initiation or the tipping point of the conversion from fibrous root to storage root and its core regulators. DNB is such an analytical system to explore genome-wide dynamic gene network and to dissect the critical transitions with their leading regulators during developmental process. In contrast, conventional transcriptomic analyses have provided insights into temporal gene expression associated with sweet potato root development (Wang et al., 2015, Firon et al., 2013, Dong et al., 2019); however, the approach is limited by a number of steady-state gene expression profiles. In this study, DNB analysis yielded a considerably more comprehensive gene sets associated with the early developmental stages compared to the previous transcriptomic studies. Most importantly, we have identified the critical state of storage root initiation and validated that *IbNAC083* is a core regulator of DNB members and is significant to storage root initiation.

The expression data throughout the seven root development stages exhibited high reproducibility and differential expression during the formation and development of sweet potato storage root. On the basis of PCA analysis, the root developmental stages were clustered into four prominent groups, signifying the differences in the gene expression profiles from one stage to another (Figure 2a). These clusters depicted similar kind of gene expression during the progression from fibrous roots to mature storage roots. Furthermore, the biological functions of these differently expressed genes in different developmental stages were drawn by GO analysis, which highlighted the significant changes in various metabolic process e.g., carbohydrate metabolic process, cell wall, transcription regulator activity,

protein metabolic process, secondary metabolic process and response to stress and these findings are in line with the previous findings (Firon et al., 2013). The data obtained during the root developmental process validated and established a chronology of gene expression events and revealed that the onset of down-regulation enriched biological functions preceded that of activation. The first state conversion was started from S8 to S10 stage and represented by the transcriptional regulators (Figure 3b, c), which is consistent with the apparent changes in lignin and starch contents during this period (Figure 1c, d). In our findings, hormonal metabolism and hormone-mediated signaling pathways were first targets for activation, followed by primary and secondary metabolism, development process, cell wall development, and cell differentiation (Figure 3c). Previously, the hormonal activation and their functions during storage root developmental process were also highlighted (Dong et al., 2019). These observations correlated well with the activation of AP2/ERF TF genes, which play crucial roles in metabolism and development process, and the overrepresentation of AP2/ERF regulatory motifs in the later stages. The TF-binding motifs of MYB and bZIP, which are linked to secondary metabolism, stress signaling and development, were only overrepresented in down-regulated genes, which are in good agreement with the previous studies about the functions of these TFs (Jakoby et al., 2002, Martin and PazAres, 1997). By integrating the TF regulatory motif overrepresentation data with our chronological root developmental network, we established the potential causal regulatory relationships between TFs and target subnetworks (Figure 3d). Approximately 40% of these TFs were found to be key regulators in root growth and development, emphasizing the high reliability of our method in the detection of biological roles of novel genes in the root developmental network.

To further investigate the mechanisms underlying the process of storage root formation and development, gene coexpression network analysis was conducted and we determined gene modules involving a mass of TFs related to developmental stages from fibrous root to mature storage root (Figure 4). These TFs can play synergistic roles in regulating the expression of coexpressed genes within each module. The results of GO analysis emphasized the significant functions of several biological processes during root developmental progression. Furthermore, we established the transcriptional regulation networks connecting TFs with their putative regulatory motifs and target genes (TF-regulatory motifs-coexpressed genes) for the three (S8, S10 and S12) critical periods of root

development that are supposed to play a decisive role in storage root initiation in sweet potato. Several members of these regulatory networks were found to be involved in different aspects of root development in different plants (Li et al., 2020b, Cai et al., 2014, Sakaoka et al., 2018, Romano et al., 2012, Huang et al., 2016, Petricka et al., 2012, Randall et al., 2015, Woerlen et al., 2017, Bomal et al., 2008). Our results indicated that analysis of transcriptional regulatory networks except for the establishment of coexpression modules can be extremely useful to investigate the molecular mechanisms of root development. However, to illustrate the details of these GRNs, it is necessary to conduct further functional investigation on each component in the network.

In order to determine the potential biomarkers of the critical swelling stage and better investigate the molecular mechanisms governing storage root initiation, we have performed the DNB method and identified S10 stage as the tipping point of root swelling initiation based on this method (Figure 5a), which is also consistent with the root development progression (Figure 1a, b) and the dynamics of gene expression (Figure 2c, Figure S1b and Figure 3b, c). Furthermore, *IbNAC083* was found to be one of regulators in DNB-associated network and might have an important influence on storage root initiation. Downregulation of *IbNAC083* significantly inhibited storage root initiation (Figure 5b-f). Previously, leading into the lignification in the initiating storage roots, *Lc* transgenic sweet potato affected the storage root development (Wang et al., 2016). Therefore, lignification could be the limited factor for initiating storage roots. In *Arabidopsis*, *IbNAC083* yields a TF belonging to NAC gene family, which can negatively regulate xylem vessel formation by interacting with *VND7* (Yamaguchi et al., 2010). *IbNAC083* is also found to act with *COR/RD* genes to affect leaf senescence through integrating abscisic acid signals (Yang et al., 2011b). Recently, *IbNAC083* is identified as a root hair cell enriched TF gene by the analysis of accessible chromatin regions throughout various plant species and cell types (Maher et al., 2018). Furthermore, the function of *IbNAC083* in the DNB-associated network was uncovered and the genes and biological functions that can be influenced by *IbNAC083* during storage root initiation were revealed (Figure 6a-c, Figure S5a-d and Table S7). By RNA-Seq, we found that several known root development related genes can be regulated by *IbNAC083* in a cascading manner (Figure 6d). These results confirmed that *IbNAC083* played an important role in initiating root swelling process by regulating multiple metabolic and signaling pathways (Figure 6e).

In summary, our work furnishes new insights into the dynamics and architecture of the root development regulatory network and a valuable data set for mining other genes associated with root growth and development in root crops like sweet potato. Our work is another successful example of identifying the tipping point of a critical developmental transition in plants using DNB. In particular, DNB identified *IbNAC083* as an early indicator and a key regulator of the initiation of storage roots in sweet potato.

EXPERIMENTAL PROCEDURES

Plant materials

Sweet potato (*Ipomoea batatas* L.) Cv. Taizhong6 plants were cultivated in early May in the Wushe Plantation for Transgenic Crops, Shanghai, China (31°13948.0099 N, 121°28912.0099E). The wild-type and transgenic sweet potato plants were planted with density of 50 cm by 50 cm (length by width), and each line had more than 6 plants. Sweet potato grew up under clay soils without fertilizer on rainfall conditions for 20 weeks. Fibrous roots at two stages (S4 and S8; root diameters of 1.5 mm and 2 mm respectively), pencil roots at two stages (S10 and S12; root diameters of 3.5 mm and 5 mm respectively) and storage roots at three stages (S14, S16 and S20; root diameters of 10 mm, 15 mm and 25 mm respectively) were collected in early October to cover the entire storage root initiation and development processes (Wang, Yang et al. 2016). Roots in each development stage have four independent biological replicates. These materials were separated into three parts: one part was rapidly frozen in liquid nitrogen and subsequently stored at -80°C for RNA isolation; and the other part was dried at 80°C for 48 h to acquire a stable dry weight (DW), which was used for analysis of lignin, starch and sugar content; and the last part was used immediately for anatomical observations.

Plasmid and *Agrobacterium*-mediated sweet potato transformation and phenotypic characterization of *IbNAC083*-RNAi transgenic plants

Sweet potato cDNA was used to obtain the ORF of *IbNAC083* (729 bp). The pRNAi-DFR vector was utilized to construct the pRNAi-*IbNAC083* binary vector to express hairpin RNA of the 250-bp *IbNAC083* fragment (451–700 bp) (Wang et al., 2013) by using the primers *IbNAC083*-KpnI (5'-CGGGGTACCAACGAGAATTGGGTACTCTG-3', KpnI site in bold), *IbNAC083*-ClaI

(5'-CCATCGATTACTGCAGCTGCACTCTCT-3', ClaI site in bold), *IbNAC083*-BamHI (5'-CGGGATCCAACGAGAATTGGGTACTCTG-3', BamHI site in bold) and *IbNAC083*-XhoI (5'-CCGCTCGAGTACTGCAGCTGCTACTCTCT-3', XhoI site in bold). Then, pRNAi-*IbNAC083* was transferred into *Agrobacterium tumefaciens* strain LBA4404 to transform sweet potato (Yang et al., 2011a). After obtaining transgenic plants, *IbNAC083* expression was detected by RT-qPCR and was normalized to the sweet potato β -Actin internal control gene.

The phenotypes of the wild-type (WT) and *IbNAC083*-RNAi sweet potato were studied under field conditions in the Wushe Plantation. We recorded the field characteristics of root at different developmental stages and the yield was examined as the average root weight of nine individual plants per line.

Anatomical observations

We used 4% neutral-buffered formalin to fix the cross-sections from the middle of fibrous roots (S4 and S8), pencil roots (S10 and S12) and storage roots (S14 and S16) of sweet potato for 24 h and then utilized paraffin wax to embed these cross-sections. We cut 15 μ m thick sections and placed these samples on silane-coated slides to fix them. These sections were dewaxed and rehydrated after baking for 12 h at 37°C. Then, the samples were incubated with toluidine blue (0.05%) for 3 min at 25°C and were washed with water to remove the staining solution. Finally, an Olympus BX51 microscope (Olympus, Japan) was used to observe the tissues.

Analysis of lignin, starch and sugar contents

Lignin content was analyzed as previously described (Gui et al., 2019). Furthermore, we accurately weighed 30 mg dried samples and put them into 5 ml tubes, then adding 0.7 ml ethanol (80%). After shaking and mixing thoroughly, these samples were placed at 70 °C for 2 h. Then, we added 0.7 ml HPLC-grade water and 0.7 ml chloroform into the tube and vibrated these samples several times, followed by centrifuged at 12,000 \times g for 10 min. The sediments were used to examine starch content while the supernatants were collected to analyze the content of soluble sugars. We washed the sediments three times using 80% ethanol, and utilized the Total Starch Assay Kit (Megazyme, Wicklow, Ireland) to examine total starch contents. We transferred 0.7 ml supernatant to 1.5 ml tube

and added 0.7 ml chloroform into each sample. After shaking and mixing thoroughly, these samples were centrifuged at $12,000 \times g$ for 10 min and then we transferred 0.5 ml supernatant into a glass tube to analyze content of each sugar component using HPLC. The sugar-separation method was according to the manufacturer's instruction with some modification; the Agilent technologies HPLC column (ZORBAX Carbohydrate column; 4.6×150 mm, $5 \mu\text{m}$) was utilized with a differential refraction detector. We used 75% acetonitrile as mobile phase; the flow velocity was 0.8 ml/min and the column temperature was 35°C . The retention times of sugar standards were used to identify each sugar components and the sugar content was obtained based on the external standard curve. Data from at least three technical replicates are presented as the mean \pm SD.

Illumina sequencing, read mapping and differential expression analysis of genes

For RNA-sequencing analysis, total RNA was isolated from the middle sections of fibrous roots (S4 and S8), pencil roots (S10 and S12) and storage roots (S14, S16 and S20) using the RNeasy Mini Kit (Qiagen) with the protocol provided by the manufacturer. The RNA Integrity Number (RIN) was used to analyze RNAs quality using an Agilent 2100 Bioanalyzer and Nanodrop 2000 (Thermo Scientific, Waltham, United States). RNA-Seq library preparation and sequencing were conducted by Majorbio Co., LTD (Shanghai, China). The Illumina TruSeq RNA Sample Prep Kit was used to prepare all the 28 libraries (7 samples in four biological replicates), and these samples were sequenced by Illumina platform (Novaseq 6000) to generate 150-nucleotide-long paired-end sequence reads. We used various quality parameters to assess the raw sequence data and used the NGS QC Toolkit (v2.3) (Patel and Jain, 2012) to filter the high-quality reads. Mapping onto the sweet potato genome (Yang et al., 2017) of filtered high-quality reads was performed by TopHat (v2.0.0). The mapped reads were processed by StringTie (v1.3.3b) to generate a transcription assembly. The TPM values of each sweet potato gene were obtained by RSEM (v1.3.1) using the mapped output. Two R packages, i.e., corrp1t and prcomp utilities, were used to perform hierarchical clustering and principal component analysis (PCA) analysis, respectively. The TPM values were used to determine differentially expressed genes with false discovery rate (q -value) ≤ 0.05 and fold change > 2 through DESeq2 (v1.30.0) (Love et al., 2014). SS scoring algorithm was used to identify the developmental stage-specific/preferential genes

through comparing the transcriptional level of one gene at a given stage with its maximum transcriptional level in other stages (Zhan et al., 2015). For a specific gene i , its expression values in 7 stages are denoted as $EV_i = (E_1^i, E_2^i, E_3^i, \dots, E_7^i)$, and SS score of the gene in stage j is defined as: $SS(i, j) = 1 - \frac{\max E_k^i}{E_j^i}$, where $1 \leq k \leq 7, k \neq j$. Therefore, higher SS score of one gene at a specific stage indicates its more preferential expression in the corresponding stage. For a particular gene list, we calculated row-wise Z-scores and used heatmap2 of R package to draw heatmaps.

For RNA-sequencing analysis of WT and *IbNAC083*-RNAi transgenic plants, the RNeasy Mini Kit (Qiagen) was used to isolate total RNAs of initial swelling roots of WT (S12-S14) and transgenic plants (S12-S14) according to the protocol provided by the manufacturer. Illumina platform (Novaseq 6000) was used to sequence all the six libraries (2 samples with three biological replicates per sample) to generate sequence reads. Other processes and analyses were the same as above.

GO enrichment analysis

Cytoscape (BiNGO plug-in) (Maere et al., 2005) was used to conduct the Gene ontology (GO) enrichment analysis of particular gene sets. The P -value of each represented GO category was adjusted by Benjamini Hochberg error correction method. The GO terms with adjusted P -value of ≤ 0.05 were considered to be remarkable overrepresented. The background for the GO analysis was the total protein coding genes of sweet potato.

RT-qPCR analysis

To validate the results of RNA-Seq, we conduct RT-qPCR assay using four biological replicates for each tissue sample and at least three technical replicates of each biological replicate. Furthermore, to quantify the gene expression levels of WT and *IbNAC083*-RNAi transgenic plants, total RNA was isolated from the middle sections of roots of WT (S12-S14) and transgenic plants (S12-S14) using at least three biological replicates per line and three technical replicates of each sample. After the RNA quality was confirmed, 2 μ g mRNA from each sample was reverse transcribed to cDNA. RT-qPCR analyses were conducted according to the previous study (Xu et al., 2013). Primer Express (v3.0) software was used to design the gene-specific primers (Table S10). Each gene was normalized to the

β -Actin internal control gene, and the fold change was calculated using the $2^{-\Delta\Delta CT}$ method.

TF family and promoter motif analysis

To identify which TF families are overrepresented among DEGs at each developmental stage, we analyzed for enrichment of 58 TF families contained in the TF database PlantTFDB version 4.0 (Jin et al., 2017). Cumulative hypergeometric distribution was used to analyze the enriched TF families within a gene list, and the total protein coding genes were treated as the background. *P*-values were adjusted using the Bonferroni method.

To predict directional interactions in transcriptional states of the root developmental gene regulatory network, TFs of sweet potato were first predicted by checking “Best hit in *Arabidopsis thaliana*” in PlantTFDB, and the matching relationship between a given sweet potato TF and its putative binding motif was also obtained. Next, we analyzed 1-kb upstream sequences of all the genes in each gene set and identified significantly enriched DNA sequence motifs by HOMER (v 4.8.3) based on the high-quality TF binding motifs collected from PlantTFDB database. Further, their association/binding with the TFs included in the same transcriptional state was identified by the above obtained matching relationships.

Co-expression network analysis for constructing modules

The WGCNA (Zhang and Horvath, 2005a, Langfelder and Horvath, 2008) package was used to establish the co-expression network. We obtained a matrix of pairwise spearman correlation coefficients (SCCs) between all gene pairs according to $\log_2(1 + TPM)$ values and converted it to an adjacency matrix using the formula: connection strength (adjacency value) = $|(1 + correlation)/2|^\beta$. Here, based on the scale-free topology criterion, a soft threshold β value of 15 was selected. Then, TOM similarity algorithm was utilized to transform the above adjacency matrix to a topological overlap (TO) matrix (Zhang and Horvath, 2005b), and hierarchical clustering dendrogram was generated based on TO similarity and was cut by the dynamic tree-cutting algorithm to get the stable clustering groups. The module eigengene (ME) of each module was computed by PCA. To analyze the relationship of module with phenotypes, the correlation between each ME and the data of these characteristics was calculated. To determine the association of module with stage-specific expression, we determined the

correlation between each ME with the binary indicator (stage = 1 and all other samples = 0) as described (Downs et al., 2013). A positive correlation indicates that genes in a module have higher/preferential expression in a particular stage relative to all other samples. Additionally, to predict directional interactions in the transcriptional regulatory network associated with the coexpressed modules, the same method as the “TF family and promoter motif analysis” part was performed. To obtain GO terms, FIMO (Grant et al., 2011) was used to screen genes, of which promoters contain a given significantly enriched motif in one module/gene set. A motif with at least one match with a $P\text{-value} \leq 10^{-4}$ in a particular promoter was considered to the existence of the motif in the corresponding promoter. Subsequently, these selected genes were used to perform GO enrichment analysis.

DNB analysis

Many investigations about complex biological processes (e.g., complex diseases, development processes, and cell cycle processes) have indicated that the progression of a complex biological process is not always smooth phenomena with linear changes but have occasionally drastic and nonlinear transitions (Liu et al., 2014, Zhang et al., 2019). Such a transition has an important influence on biological processes due to its qualitative alterations of biological system state. In particular, determining the tipping point just before this transition can not only reveal the molecular mechanism of this dynamical process but also infer its core regulators with the corresponding regulatory network. Therefore, to uncover the dynamical biomarkers and analyze the molecular mechanisms of swelling initiation of sweet potato storage roots, we analyzed the RNA-Seq data by using the DNB method. According to the nonlinear dynamical theory, a biological system is near the tipping point when there is a dominant gene set, i.e., DNB, which meet the following three necessary conditions of gene expressions (Chen et al., 2012, Li et al., 2017, Li et al., 2014, Liu, 2013, Yang et al., 2018, Liu et al., 2019a, Liu et al., 2019b):

- (1) The transcript levels of DNB members are highly fluctuated, represented by coefficient values of variation (CV_{in});
- (2) The correlation among the DNB genes become dramatically increased, represented by absolute Pearson correlation coefficient (PCC_{in});

(3) The association between DNB genes and the other genes become drastically decreased, indicated by the absolute value of PCC (PCC_{out}).

To consider all the above conditions, a criticality index (CI) can be defined as:

$$CI = \frac{PCC_{in}}{PCC_{out}} CV_{in}$$

Here, CV_{in} , PCC_{in} , and PCC_{out} are all average values. Based on the above conditions and the criticality index, genes with CV values lower than 70% percentile throughout all the time points were filtered out, and the following steps were conducted to identify DNB members/genes at each time point:

- (1) Obtaining gene modules by clustering the selected genes, and the distance is defined as $1 - |PCC|$ and the cutoff is set to 0.1;
- (2) Computing the CI of each module;
- (3) Selecting the maximum CI module at each time point, and considering it as the potential DNB module;
- (4) Selecting the maximum CI potential module of all the time points through comparing all the candidate modules, and this potential module is the expected DNB module (with all genes in the module as DNB members) and the corresponding stage is the tipping point.

Clearly, DNB method is mainly based on “differential associations among genes” (differential network or the second-order statistics), rather than “differential expressions of genes” (differential genes or the first-order statistics) in the most of the traditional methods.

STRING database (<http://string-db.org>) and Cytoscape software (<http://www.cytoscape.org/>) were used to build molecular interactions (protein-protein interactions) network and visualization, respectively (Szklarczyk et al., 2015, Shannon et al., 2003). In the network, the nodes indicate genes and the edges indicate interactions. For a particular gene list, we calculated root developmental stage-wise Z-scores as the expression level of corresponding genes.

Ranking scheme for core regulators of DNB members

We ranked the core regulators of DNB genes near the critical stage S10 based on the following criteria with four priorities.

- (1) Priority one. We ranked the regulators of DNB members according to their significance to the

network. Core TFs are regarded as playing dominant roles in the molecular network composed of DNB genes and their predicted TFs during root swelling initiation. Then, these genes were mapped into the network and the total number of DNB members directly connected with each TF member was calculated individually. This criterion is indicated as a ratio of target DNB genes belonging to DEGs from S8 to S12 stages to the total target DNB genes regulated by each TF gene.

- (2) Priority two. We required that TFs need to be differentially expressed from S8 to S12 stages to regulate the expression of target genes, although this would ignore the regulatory effect of non-differential expression of some TFs on target genes, such as protein modification. This criterion represents whether or not a TF belongs to DEGs from S8 to S12 stages.
- (3) Priority three. To identify the TFs that play crucial regulatory roles in the initial expansion process of storage root, we required that key TFs should be one of the enriched motifs associated TFs regulating DEGs from S8 to S10 stages (Figure 3D). This criterion represents whether or not a TF belongs to the enriched motifs associated TFs regulating DEGs from S8 to S10 stages (Figure 3D).
- (4) Priority four. To explore the key regulators in the initial swelling stage of storage root, we selected TFs that might play crucial roles in early stage of tipping point, i.e., S8 stage. This criterion represents whether or not a TF belongs to the enriched motifs associated TFs in the S8 module (Figure 4B).

GUS staining and subcellular localization of IbNAC083

To study the tissue localization of IbNAC083, the promoter of *IbNAC083* (2573bp) fused to a *uidA* gene was constructed into pCAMBIA1300 with *Pst* I and *Bam*H I, and transformed to Arabidopsis through *Agrobacterium*-mediated DNA transformation. The positive transgenic lines were selected by kanamycin resistance for GUS staining. GUS staining of root in Arabidopsis was conducted according to a previous study (Yu et al., 2013). For subcellular localization experiments, a vector yielding IbNAC083-GFP fusion proteins was constructed with the CaMV 35S promoter and was transferred into tobacco leaf by *Agrobacterium*-mediated transformation. Finally, the leaf was observed under an Olympus FV1000 microscope (Olympus, Japan). The primers used in this study are listed in Table S10.

Statistical analysis

Independent samples Student's *t*-test was conducted using SPSS software, version 17 (SPSS Inc., Chicago, IL, USA). An alpha value of $P < 0.05$ was considered statistically significant.

ACCESSION NUMBERS

The RNA-seq data are available in the NCBI Sequence Read Archive under accession number PRJNA647694.

DATA AVAILABILITY STATEMENT

All relevant data can be found within the manuscript and its supporting materials.

ACKNOWLEDGEMENTS

This work was supported by National Key R&D Program of China (Nos. 2017YFA0505500 and 2018YFD1000705), Priority Research Program of the Chinese Academy of Sciences (No. XDB38040400), the National Natural Science Foundation of China (Nos. 31930022, 12026608 and 31771476), and Japan Science and Technology Agency Moonshot R&D (No. JPMJMS2021).

AUTHOR CONTRIBUTIONS

Luonan Chen, Peng Zhang, and Shutao He designed and conceived this project; Shutao He performed the analysis of RNA-Seq data; Xiaomeng Hao, Yinliang Wu, Hongxia Wang, Yandi Zhang, Xiaofeng Bian, Weijuan Fan, Minhao Yin and Shutao He executed the experiment; Shutao He and Xiaomeng Hao prepared the figure and drafted the manuscript; Luonan Chen, Peng Zhang, Ling Yuan, Shutao He and Hongxia Wang analyzed the data and revised the manuscript with input from the other authors. All authors dedicated to and approved the final manuscript.

CONFLICT OF INTEREST

The authors declare no conflict of interest.

SUPPORTING INFORMATION

Additional Supporting Information may be found in the online version of this article.

Figure S1. Preferential/stage-specific expression of genes at different developmental stages of sweet potato roots.

Figure S2. Correlation between expression profiles of selected genes obtained from RNA-Seq and

RT-qPCR analysis.

Figure S3. Circos plots of developmental series expression profiles in comparison to previously published sweet potato root transcriptome data

Figure S4. Expression profile and subcellular localization of IbNAC083.

Figure S5. Changes in lignin and starch contents and related metabolic gene expression profile in the initial swelling roots of WT (S19-S20) and *IbNAC083*-RNAi transgenic plants (S13-S14).

Table S1. Summary of the transcriptome data in sweet potato roots.

Table S2. The novel gene sequences of sweet potato.

Table S3. TPM values for all the detected genes in sweet potato roots.

Table S4. SS scores for all preferentially expressed genes in sweet potato roots.

Table S5. Differentially expressed genes (DEGs) between different root developmental stages of sweet potato.

Table S6. Gene modules identified by WGCNA.

Table S7. The relationships between members in IbNAC083-centered DNB network.

Table S8. Summary of the transcriptome data of WT and IbNAC083-RNAi initial swelling roots.

Table S9. TPM values of DEGs between WT and IbNAC083-RNAi initial swelling roots.

Table S10. Primer pairs used in this study.

REFERENCES

BELEHU, T., HAMMES, P. S. & ROBBERTSE, P. J. 2004. The origin and structure of adventitious roots in sweet potato (*Ipomoea batatas*). *Australian Journal of Botany*, 52, 551-558.

BOMAL, C., BEDON, F., CARON, S., MANSFIELD, S. D., LEVASSEUR, C., COOKE, J. E. K., BLAIS, S., TREMBLAY, L., MORENCY, M. J., PAVY, N., GRIMA-PETTENATI, J., SEGUIN, A. & MACKAY, J. 2008. Involvement of *Pinus taeda* MYB1 and MYB8 in phenylpropanoid metabolism and secondary cell wall biogenesis: a comparative in planta analysis. *Journal of Experimental Botany*, 59,

3925-3939.

BONKE, M., THITAMADEE, S., MAHONEN, A. P., HAUSER, M. T. & HELARIUTTA, Y. 2003. APL regulates vascular tissue identity in Arabidopsis. *Nature*, 426, 181-186.

BROWN, D. E., RASHOTTE, A. M., MURPHY, A. S., NORMANLY, J., TAGUE, B. W., PEER, W. A., TAIZ, L. & MUDAY, G. K. 2001. Flavonoids act as negative regulators of auxin transport in vivo in Arabidopsis. *Plant Physiology*, 126, 524-535.

CAI, X. T., XU, P., ZHAO, P. X., LIU, R., YU, L. H. & XIANG, C. B. 2014. Arabidopsis ERF109 mediates cross-talk between jasmonic acid and auxin biosynthesis during lateral root formation. *Nature Communications*, 5.

CHEN, L. N., LIU, R., LIU, Z. P., LI, M. Y. & AIHARA, K. 2012. Detecting early-warning signals for sudden deterioration of complex diseases by dynamical network biomarkers. *Scientific Reports*, 2.

CHEN, P. L., R.; LI, Y. J.; CHEN, L. N. 2016. Detecting critical state before phase transition of complex biological systems by hidden Markov model. *Bioinformatics*, 32, 2143-2150.

DEVAIAH, B. N., KARTHIKEYAN, A. S. & RAGHOTHAMA, K. G. 2007. WRKY75 transcription factor is a modulator of phosphate acquisition and root development in arabidopsis. *Plant Physiology*, 143, 1789-1801.

DONG, T. T., ZHU, M. K., YU, J. W., HAN, R. P., TANG, C., XU, T., LIU, J. R. & LI, Z. Y. 2019. RNA-Seq and iTRAQ reveal multiple pathways involved in storage root formation and development in sweet potato (*Ipomoea batatas* L.). *Bmc Plant Biology*, 19.

DOWNS, G. S., BI, Y. M., COLASANTI, J., WU, W. Q., CHEN, X., ZHU, T., ROTHSTEIN, S. J. & LUKENS, L. N. 2013. A Developmental Transcriptional Network for Maize Defines Coexpression Modules.

Plant Physiology, 161, 1830-1843.

EYSHOLDT-DERZSO, E. & SAUTER, M. 2017. Root Bending Is Antagonistically Affected by Hypoxia and ERF-Mediated Transcription via Auxin Signaling. *Plant Physiology*, 175, 412-423.

FARINATI, S., DALCORSO, G., VAROTTO, S. & FURINI, A. 2010. The Brassica juncea BjCdR15, an ortholog of Arabidopsis TGA3, is a regulator of cadmium uptake, transport and accumulation in shoots and confers cadmium tolerance in transgenic plants. *New Phytologist*, 185, 964-978.

FIRON, N., LABONTE, D., VILLORDON, A., KFIR, Y., SOLIS, J., LAPIS, E., PERLMAN, T. S., DORON-FAIGENBOIM, A., HETZRONI, A., ALTHAN, L. & NADIR, L. A. 2013. Transcriptional profiling of sweetpotato (*Ipomoea batatas*) roots indicates down-regulation of lignin biosynthesis and up-regulation of starch biosynthesis at an early stage of storage root formation. *Bmc Genomics*, 14.

GARCIA, M. N. M., STRITZLER, M. & CAPIATI, D. A. 2014. Heterologous expression of Arabidopsis ABF4 gene in potato enhances tuberization through ABA-GA crosstalk regulation. *Planta*, 239, 615-631.

GRANT, C. E., BAILEY, T. L. & NOBLE, W. S. 2011. FIMO: scanning for occurrences of a given motif. *Bioinformatics*, 27, 1017-1018.

GUI, J. S., LUO, L. F., ZHONG, Y., SUN, J. Y., UMEZAWA, T. & LI, L. G. 2019. Phosphorylation of LTF1, an MYB Transcription Factor in Populus, Acts as a Sensory Switch Regulating Lignin Biosynthesis in Wood Cells. *Molecular Plant*, 12, 1325-1337.

GUTIERREZ, L., BUSSELL, J. D., PACURAR, D. I., SCHWAMBACH, J., PACURAR, M. & BELLINI, C. 2009. Phenotypic Plasticity of Adventitious Rooting in Arabidopsis Is Controlled by Complex Regulation of AUXIN RESPONSE FACTOR Transcripts and MicroRNA Abundance. *Plant Cell*, 21,

3119-3132.

- HACHAM, Y., HOLLAND, N., BUTTERFIELD, C., UBEDA-TOMAS, S., BENNETT, M. J., CHORY, J. & SAVALDI-GOLDSTEIN, S. 2011. Brassinosteroid perception in the epidermis controls root meristem size. *Development*, 138, 839-848.
- HUANG, Y. C., NIU, C. Y., YANG, C. R. & JINN, T. L. 2016. The Heat Stress Factor HSFA6b Connects ABA Signaling and ABA-Mediated Heat Responses. *Plant Physiology*, 172, 1182-1199.
- ITO, T., KIM, G. T. & SHINOZAKI, K. 2000. Disruption of an Arabidopsis cytoplasmic ribosomal protein S13-homologous gene by transposon-mediated mutagenesis causes aberrant growth and development. *Plant Journal*, 22, 257-264.
- JAKOBY, M., WEISSHAAR, B., DROGE-LASER, W., VICENTE-CARBAJOSA, J., TIEDEMANN, J., KROJ, T., PARCY, F. & GRP, B. R. 2002. bZIP transcription factors in Arabidopsis. *Trends in Plant Science*, 7, 106-111.
- JIA, Y. B., TIAN, H. Y., LI, H. J., YU, Q. Q., WANG, L., FRIML, J. & DING, Z. J. 2015. The Arabidopsis thaliana elongator complex subunit 2 epigenetically affects root development. *Journal of Experimental Botany*, 66, 4631-4642.
- JIANG, Z. L., LU, L. N., LIU, Y. W., ZHANG, S., LI, S. X., WANG, G. Y., WANG, P. & CHEN, L. N. 2020. SMAD7 and SERPINE1 as novel dynamic network biomarkers detect and regulate the tipping point of TGF-beta induced EMT. *Science Bulletin*, 65, 842-53.
- JIN, J. P., TIAN, F., YANG, D. C., MENG, Y. Q., KONG, L., LUO, J. C. & GAO, G. 2017. PlantTFDB 4.0: toward a central hub for transcription factors and regulatory interactions in plants. *Nucleic Acids Research*, 45, D1040-D1045.

- KIM, T. H., KUNZ, H. H., BHATTACHARJEE, S., HAUSER, F., PARK, J., ENGINEER, C., LIU, A., HA, T., PARKER, J. E., GASSMANN, W. & SCHROEDER, J. I. 2012. Natural Variation in Small Molecule-Induced TIR-NB-LRR Signaling Induces Root Growth Arrest via EDS1-and PAD4-Complexed R Protein VICTR in Arabidopsis. *Plant Cell*, 24, 5177-5192.
- KOBAYASHI, K., AWAI, K., NAKAMURA, M., NAGATANI, A., MASUDA, T. & OHTA, H. 2009. Type-B monogalactosyldiacylglycerol synthases are involved in phosphate starvation-induced lipid remodeling, and are crucial for low-phosphate adaptation. *Plant Journal*, 57, 322-331.
- KU, A. T., HUANG, Y. S., WANG, Y. S., MA, D. F. & YEH, K. W. 2008. IbMADS1 (Ipomoea batatas MADS-box 1 gene) is involved in tuberous root initiation in sweet potato (Ipomoea batatas). *Annals of Botany*, 102, 57-67.
- LANGFELDER, P. & HORVATH, S. 2008. WGCNA: an R package for weighted correlation network analysis. *Bmc Bioinformatics*, 9.
- LI, H., YAO, L., SUN, L. & ZHU, Z. 2020a. ETHYLENE INSENSITIVE 3 suppresses plant de novo root regeneration from leaf explants and mediates age-regulated regeneration decline. *Development*, 147.
- LI, M. Y., LI, C., LIU, W. X., LIU, C. H., CUI, J. R., LI, Q. R., NI, H., YANG, Y. C., WU, C. C., CHEN, C. L., ZHEN, X., ZENG, T., ZHAO, M. J., CHEN, L., WU, J. R., ZENG, R. & CHEN, L. N. 2017. Dysfunction of PLA2G6 and CYP2C44-associated network signals imminent carcinogenesis from chronic inflammation to hepatocellular carcinoma. *Journal of Molecular Cell Biology*, 9, 489-503.
- LI, M. Y., ZENG, T., WANG, Y. S. & CHEN, L. N. 2014. Detecting tissue-specific early-warning signals for complex diseases based on dynamical network biomarkers: study of type-2 diabetes by

cross-tissue analysis. *Briefings in Bioinformatics*, 15, 229-43.

LI, S. X., NAYAR, S., JIA, H., KAPOOR, S., WU, J. & YUKAWA, Y. 2020b. The Arabidopsis Hypoxia Inducible AtR8 Long Non-Coding RNA also Contributes to Plant Defense and Root Elongation Coordinating with WRKY Genes under Low Levels of Salicylic Acid. *Non-Coding RNA*, 6, 8.

LIU, R., CHEN, P., AIHARA, K. & CHEN, L. N. 2015. Identifying early-warning signals of critical transitions with strong noise by dynamical network markers. *Scientific Reports*, 5.

LIU, R., WANG, J. Z., UKAI, M., SEWON, K., CHEN, P., SUZUKI, Y., WANG, H. Y., AIHARA, K., OKADA-HATAKEYAMA, M. & CHEN, L. N. 2019a. Hunt for the tipping point during endocrine resistance process in breast cancer by dynamic network biomarkers. *Journal of Molecular Cell Biology*, 11, 649-664.

LIU, R., WANG, X. F., AIHARA, K. & CHEN, L. 2014. Early diagnosis of complex diseases by molecular biomarkers, network biomarkers, and dynamical network biomarkers. *Med Res Rev*, 34, 455-78.

LIU, R. A., K.; CHEN L. 2013. Dynamical network biomarkers for identifying critical transitions and their driving networks of biologic processes. *Quantitative Biology*, 1, 105-14.

LIU, X. P., CHANG, X., LENG, S. Y., TANG, H., AIHARA, K. & CHEN, L. N. 2019b. Detection for disease tipping points by landscape dynamic network biomarkers. *National Science Review*, 6, 775-785.

LOVE, M. I., HUBER, W. & ANDERS, S. 2014. Moderated estimation of fold change and dispersion for RNA-seq data with DESeq2. *Genome Biol*, 15, 550.

MA, J., LIU, Y. H., ZHOU, W. B., ZHU, Y., DONG, A. W. & SHEN, W. H. 2018. Histone chaperones play crucial roles in maintenance of stem cell niche during plant root development. *Plant Journal*, 95, 86-100.

MAERE, S., HEYMANS, K. & KUIPER, M. 2005. BiNGO: a Cytoscape plugin to assess overrepresentation of Gene Ontology categories in Biological Networks. *Bioinformatics*, 21, 3448-3449.

MAHER, K. A., BAJIC, M., KAJALA, K., REYNOSO, M., PAULUZZI, G., WEST, D. A., ZUMSTEIN, K., WOODHOUSE, M., BUBB, K., DORRITY, M. W., QUEITSCH, C., BAILEY-SERRES, J., SINHA, N., BRADY, S. M. & DEAL, R. B. 2018. Profiling of Accessible Chromatin Regions across Multiple Plant Species and Cell Types Reveals Common Gene Regulatory Principles and New Control Modules. *Plant Cell*, 30, 15-36.

MARTIN, C. & PAZARES, J. 1997. MYB transcription factors in plants. *Trends in Genetics*, 13, 67-73.

NAKATANI, M. 1994. In-Vitro Formation of Tuberous Roots in Sweet-Potato. *Japanese Journal of Crop Science*, 63, 158-159.

NAKATANI, M. & KOMEICHI, M. 1991. Changes in the Endogenous Level of Zeatin Riboside, Abscisic-Acid and Indole Acetic-Acid during Formation and Thickening of Tuberous Roots in Sweet-Potato. *Japanese Journal of Crop Science*, 60, 91-100.

NOH, S. A., LEE, H. S., HUH, E. J., HUH, G. H., PAEK, K. H., SHIN, J. S. & BAE, J. M. 2010. SRD1 is involved in the auxin-mediated initial thickening growth of storage root by enhancing proliferation of metaxylem and cambium cells in sweetpotato (*Ipomoea batatas*). *Journal of Experimental Botany*, 61, 1337-1349.

NOH, S. A., LEE, H. S., KIM, Y. S., PAEK, K. H., SHIN, J. S. & BAE, J. M. 2013. Down-regulation of the IbEXP1 gene enhanced storage root development in sweetpotato. *Journal of Experimental Botany*, 64, 129-142.

PATEL, R. K. & JAIN, M. 2012. NGS QC Toolkit: A Toolkit for Quality Control of Next Generation

Sequencing Data. *Plos One*, 7.

PEER, W. A., CHENG, Y. & MURPHY, A. S. 2013. Evidence of oxidative attenuation of auxin signalling.

Journal of Experimental Botany, 64, 2629-2639.

PETRICKA, J. J., WINTER, C. M. & BENFEY, P. N. 2012. Control of Arabidopsis Root Development.

Annual Review of Plant Biology, Vol 63, 63, 563-590.

POPESCU, S. C. & TUMER, N. E. 2004. Silencing of ribosomal protein L3 genes in N-tabacum reveals coordinate expression and significant alterations in plant growth, development and ribosome biogenesis. *Plant Journal*, 39, 29-44.

RANDALL, R. S., MIYASHIMA, S., BLOMSTER, T., ZHANG, J., ELO, A., KARLBERG, A., IMMANEN, J., NIEMINEN, K., LEE, J. Y., KAKIMOTO, T., BLAJECKA, K., MELNYK, C. W., ALCASABAS, A., FORZANI, C., MATSUMOTO-KITANO, M., MAHONEN, A. P., BHALERAO, R., DEWITTE, W., HELARIUTTA, Y. & MURRAY, J. A. H. 2015. AINTEGUMENTA and the D-type cyclin CYCD3;1 regulate root secondary growth and respond to cytokinins. *Biology Open*, 4, 1229-1236.

RAVI, V., NASKAR, S., MAKESHKUMAR, T., BABU, B. & P., K. B. 2009. Molecular physiology of storage root formation and development in sweet potato (*Ipomoea batatas* (L.) lam.). *J Root Crops*, 35, 1-27.

RIECHMANN, J. L. & MEYEROWITZ, E. M. 1998. The AP2/EREBP family of plant transcription factors. *Biological Chemistry*, 379, 633-646.

ROMANO, J. M., DUBOS, C., PROUSE, M. B., WILKINS, O., HONG, H., POOLE, M., KANG, K. Y., LI, E. Y., DOUGLAS, C. J., WESTERN, T. L., MANSFIELD, S. D. & CAMPBELL, M. M. 2012. AtMYB61, an R2R3-MYB transcription factor, functions as a pleiotropic regulator via a small gene network.

New Phytologist, 195, 774-786.

SAKAOKA, S., MABUCHI, K., MORIKAMI, A. & TSUKAGOSHI, H. 2018. MYB30 regulates root cell elongation under abscisic acid signaling. *Commun Integr Biol*, 11, e1526604.

SHANNON, P., MARKIEL, A., OZIER, O., BALIGA, N. S., WANG, J. T., RAMAGE, D., AMIN, N., SCHWIKOWSKI, B. & IDEKER, T. 2003. Cytoscape: a software environment for integrated models of biomolecular interaction networks. *Genome Res*, 13, 2498-504.

SILVA, A. T., RIBONE, P. A., CHAN, R. L., LIGTERINK, W. & HILHORST, H. W. M. 2016. A Predictive Coexpression Network Identifies Novel Genes Controlling the Seed-to-Seedling Phase Transition in *Arabidopsis thaliana*. *Plant Physiology*, 170, 2218-2231.

SINGH, V., SERGEEVA, L., LIGTERINK, W., ALONI, R., ZEMACH, H., DORON-FAIGENBOIM, A., YANG, J., ZHANG, P., SHABTAI, S. & FIRON, N. 2019. Gibberellin Promotes Sweetpotato Root Vascular Lignification and Reduces Storage-Root Formation. *Front Plant Sci*, 10, 1320.

SPENCE, J. A. & HUMPHRIES, E. C. 1972. Effect of Moisture Supply, Root Temperature, and Growth-Regulators on Photosynthesis of Isolated Rooted Leaves of Sweet Potato (*Ipomoea-Batas*). *Annals of Botany*, 36, 115-+.

SZKLARCZYK, D., FRANCESCHINI, A., WYDER, S., FORSLUND, K., HELLER, D., HUERTA-CEPAS, J., SIMONOVIC, M., ROTH, A., SANTOS, A., TSAFOU, K. P., KUHN, M., BORK, P., JENSEN, L. J. & VON MERING, C. 2015. STRING v10: protein-protein interaction networks, integrated over the tree of life. *Nucleic Acids Research*, 43, D447-D452.

TAN, H. J., MAN, C., XIE, Y., YAN, J. J., CHU, J. F. & HUANG, J. R. 2019. A Crucial Role of GA-Regulated Flavonol Biosynthesis in Root Growth of *Arabidopsis*. *Molecular Plant*, 12, 521-537.

- TANAKA, M., KATO, N., NAKAYAMA, H., NAKATANI, M. & TAKAHATA, Y. 2008. Expression of class I knotted1-like homeobox genes in the storage roots of sweetpotato (*Ipomoea batatas*). *Journal of Plant Physiology*, 165, 1726-1735.
- TOGARI, Y. 1950. A study of tuberous root formation in sweet potato. *Bul. Nat. Agr. Expt. Sta. Tokyo*, 68, 1-96.
- VAN GELDEREN, K., KANG, C. K., PAALMAN, R., KEUSKAMP, D., HAYES, S. & PIERIK, R. 2018. Far-Red Light Detection in the Shoot Regulates Lateral Root Development through the HY5 Transcription Factor. *Plant Cell*, 30, 101-116.
- VESTY, E. F., SAIDI, Y., MOODY, L. A., HOLLOWAY, D., WHITBREAD, A., NEEDS, S., CHOUDHARY, A., BURNS, B., MCLEOD, D., BRADSHAW, S. J., BAE, H., KING, B. C., BASSEL, G. W., SIMONSEN, H. T. & COATES, J. C. 2016. The decision to germinate is regulated by divergent molecular networks in spores and seeds. *New Phytologist*, 211, 952-966.
- VILLORDON, A. Q., LA BONTE, D. R., FIRON, N., KFIR, Y., PRESSMAN, E. & SCHWARTZ, A. 2009. Characterization of Adventitious Root Development in Sweetpotato. *Hortscience*, 44, 651-655.
- WANG, H. X., FAN, W. J., LI, H., YANG, J., HUANG, J. R. & ZHANG, P. 2013. Functional Characterization of Dihydroflavonol-4-Reductase in Anthocyanin Biosynthesis of Purple Sweet Potato Underlies the Direct Evidence of Anthocyanins Function against Abiotic Stresses. *Plos One*, 8.
- WANG, H. X., YANG, J., ZHANG, M., FAN, W. J., FIRON, N., PATTANAIK, S., YUAN, L. & ZHANG, P. 2016. Altered Phenylpropanoid Metabolism in the Maize Lc-Expressed Sweet Potato (*Ipomoea batatas*) Affects Storage Root Development. *Scientific Reports*, 6.
- WANG, Z. Y., FANG, B. P., CHEN, X. L., LIAO, M. H., CHEN, J. Y., ZHANG, X. J., HUANG, L. F., LUO, Z.

-
- X., YAO, Z. F. & LI, Y. J. 2015. Temporal patterns of gene expression associated with tuberous root formation and development in sweetpotato (*Ipomoea batatas*). *Bmc Plant Biology*, 15.
- WILSON, L. A. & LOWE, S. B. 1973. The anatomy of the root system in west Indian sweet potato (*Ipomoea Batatas* (L.) lam.) cultivars. *Ann Bot*, 37, 633-43.
- WOERLEN, N., ALLAM, G., POPESCU, A., CORRIGAN, L., PAUTOT, V. & HEPWORTH, S. R. 2017. Repression of BLADE-ON-PETIOLE genes by KNOX homeodomain protein BREVIPEDICELLUS is essential for differentiation of secondary xylem in *Arabidopsis* root. *Planta*, 245, 1079-1090.
- WOODWARD, A. W., RATZEL, S. E., WOODWARD, E. E., SHAMOO, Y. & BARTEL, B. 2007. Mutation of E1-CONJUGATING ENZYME-RELATED1 decreases RELATED TO UBIQUITIN conjugation and alters auxin response and development. *Plant Physiology*, 144, 976-987.
- WU, S. Y., XIE, Y. R., ZHANG, J. J., REN, Y. L., ZHANG, X., WANG, J. L., GUO, X. P., WU, F. Q., SHENG, P. K., WANG, J., WU, C. Y., WANG, H. Y., HUANG, S. J. & WAN, J. M. 2015. VLN2 Regulates Plant Architecture by Affecting Microfilament Dynamics and Polar Auxin Transport in Rice. *Plant Cell*, 27, 2829-2845.
- XU, J., DUAN, X. G., YANG, J., BEECHING, J. R. & ZHANG, P. 2013. Enhanced Reactive Oxygen Species Scavenging by Overproduction of Superoxide Dismutase and Catalase Delays Postharvest Physiological Deterioration of Cassava Storage Roots. *Plant Physiology*, 161, 1517-1528.
- YAMAGUCHI, M., MITSUDA, N., OHTANI, M., OHME-TAKAGI, M., KATO, K. & DEMURA, T. 2011. VASCULAR-RELATED NAC-DOMAIN 7 directly regulates the expression of a broad range of genes for xylem vessel formation. *Plant Journal*, 66, 579-590.

-
- YAMAGUCHI, M., OHTANI, M., MITSUDA, N., KUBO, M., OHME-TAKAGI, M., FUKUDA, H. & DEMURA, T. 2010. VND-INTERACTING2, a NAC Domain Transcription Factor, Negatively Regulates Xylem Vessel Formation in Arabidopsis. *Plant Cell*, 22, 1249-1263.
- YANG, B. W., LI, M. Y., TANG, W. Q., LIU, W. X., ZHANG, S., CHEN, L. N. & XIA, J. L. 2018. Dynamic network biomarker indicates pulmonary metastasis at the tipping point of hepatocellular carcinoma. *Nature Communications*, 9.
- YANG, J., BI, H. P., FAN, W. J., ZHANG, M., WANG, H. X. & ZHANG, P. 2011a. Efficient embryogenic suspension culturing and rapid transformation of a range of elite genotypes of sweet potato (*Ipomoea batatas* [L.] Lam.). *Plant Science*, 181, 701-711.
- YANG, J., MOEINZADEH, M. H., KUHL, H., HELMUTH, J., XIAO, P., HAAS, S., LIU, G., ZHENG, J., SUN, Z., FAN, W., DENG, G., WANG, H., HU, F., ZHAO, S., FERNIE, A. R., BOERNO, S., TIMMERMANN, B., ZHANG, P. & VINGRON, M. 2017. Haplotype-resolved sweet potato genome traces back its hexaploidization history. *Nat Plants*, 3, 696-703.
- YANG, S. D., SEO, P. J., YOON, H. K. & PARK, C. M. 2011b. The Arabidopsis NAC Transcription Factor VNI2 Integrates Abscisic Acid Signals into Leaf Senescence via the COR/RD Genes. *Plant Cell*, 23, 2155-2168.
- YU, L. L., SUN, J. Y. & LI, L. G. 2013. PtrCel9A6, an Endo-1,4--Glucanase, Is Required for Cell Wall Formation during Xylem Differentiation in Populus. *Molecular Plant*, 6, 1904-1917.
- ZHAN, J. P., THAKARE, D., MA, C., LLOYD, A., NIXON, N. M., ARAKAKI, A. M., BURNETT, W. J., LOGAN, K. O., WANG, D. F., WANG, X. F., DREWS, G. N. & YADEGARIA, R. 2015. RNA Sequencing of Laser-Capture Microdissected Compartments of the Maize Kernel Identifies

Regulatory Modules Associated with Endosperm Cell Differentiation. *Plant Cell*, 27, 513-531.

ZHANG, B. & HORVATH, S. 2005a. A general framework for weighted gene co-expression network analysis. *Statistical Applications in Genetics and Molecular Biology*, 4.

ZHANG, B. & HORVATH, S. 2005b. A general framework for weighted gene co-expression network analysis. *Stat Appl Genet Mol Biol*, 4, Article17.

ZHANG, F. P., LIU, X. P., ZHANG, A. D., JIANG, Z. L., CHEN, L. N. & ZHANG, X. J. 2019. Genome-wide dynamic network analysis reveals a critical transition state of flower development in Arabidopsis. *Bmc Plant Biology*, 19.

FIGURE LEGENDS

Figure 1. Physiological changes in different developmental stages of sweet potato.

(a) Morphology of sweet potato roots at different developmental stages.

(b) Transverse sections of sweet potato roots at different developmental stages after staining with toluidine blue. Abbreviation: CT, cortex; SXY, secondary xylem; PX, primary xylem; CA, cambium; SM, secondary meristem; AM, anomalous meristem; PC, parenchyma cell.

(c-e) Variation in lignin (c), starch (d) and sugar (e) contents of sweet potato roots at different developmental stages. CWM indicates cell wall material and DW indicates dry weight. Error bars indicates standard error (n =12).

Figure 2. Global differences in the transcriptome dynamics during root development of sweet potato.

(a) Principal component analysis (PCA) plot showing clustering of transcriptomes of sweet potato roots at different developmental stages.

(b) Biological functions that can best distinguish these samples at different developmental stages, analyzed by Gene ontology (GO) enrichment of genes with the largest load (positive value) and genes with the smallest load (negative value) in PCA.

(c) Unsupervised hierarchical clustering of transcriptomes of sweet potato roots at different developmental stages.

Figure 3. Chronology of sweet potato root developmental transcriptional reprogramming.

(a) Circos plots of developmental series expression profiles in comparison to previously published sweet potato root transcriptome data (Wang, Fang et al. 2015), as indicated underneath the plot. The stacked histograms indicate differential expression. The second to seventh circles indicate DEGs of S8-S4, S10-S8, S12-S10, S14-S12, S16-S14 and S20-S16, respectively. Genes differentially expressed in both datasets are marked by connecting bands (colors indicate first developmental stage of differential expression in our study). Each section within the circus plot represents a set of 500 DEGs.

(b) Enriched gene ontology (GO) terms of first down- and up-regulated genes at different stages of root development. The color scale at the bottom represents significance (corrected *P*-value).

(c) Analysis of the major transcriptional states in the root developmental gene regulatory network of sweet potato. DEGs were divided into four sets according to their function as regulator or non-regulator (regulated), and their expression pattern being up- (red) or down-regulated (blue) over time. Transcriptional states are indicated by boxes, aligned on the timeline. DEGs are assigned to the states according to the time point where they were differentially expressed; indicated are overrepresented functional categories (F). Colored squares indicate known TF DNA-binding motifs overrepresented in gene promoters (hypergeometric distribution; *P*-value ≤ 0.001). Pie charts indicate the proportion of TF gene families. Abbreviation: Develop., development; Reg., regulation; Str., response to stress; Metab., Metabolism; Phos., protein phosphorylation; Diff., differentiation.

(d) Predicted directional interactions in transcriptional states of the root developmental gene regulatory network. The promoter sequences of genes associated with a transcriptional state were tested for overrepresentation of DNA motifs shown to be bound to TFs that are differentially transcribed during root development. Each TF with a known motif is represented by a colored circle, and is plotted at the time point that its corresponding gene is first differentially expressed. Each regulated transcriptional state is represented by a square and plotted in time according to its onset (red and blue squares

indicate up- and down-regulated transcriptional states, respectively). An edge between a TF and a transcriptional state only indicates significant enrichment of the corresponding binding motif in that state, not the direction of regulation (positive regulation or negative regulation). The size of each TF node is proportional to the number of states in which its binding site is overrepresented. To aid interpretation of the network, nodes are grouped and colored according to the transcriptional state where they first become differentially expressed.

Figure 4. Analysis of transcription regulatory modules related to root development of sweet potato.

(a) Correlation heatmap of module eigenvalues with root development stages and physiological phenotypes. Pearson correlation coefficient and *P*-value of each module with different stages and phenotypes are given and colored according to the score.

(b-d) Expression profile and transcriptional regulatory network associated with the coexpressed modules at S8 (b), S10 (c) and S12 (d) stages. Heatmaps show the expression profile of all the coexpressed genes in the modules (labeled on top). The color scale represents Z-score. Bar graphs (below the heatmaps) show the consensus expression pattern of the coexpressed genes in each module. The predicted transcriptional regulatory network [significantly enriched transcription factor (TF)-binding sites along with the associated TFs and enriched gene ontology (GO) terms] associated with the coexpressed gene sets at S8, S10 and S12 stages of root development are given. The significantly enriched *cis*-regulatory motifs (green triangle) and GO terms (blue hexagons) within the given set of genes were linked by pink lines. The TFs are represented by magenta circles. Edges represent known interactions between the *cis*-regulatory motifs and TFs.

Figure 5. *IbNAC083* ranked as one core regulators of DNB members to promote storage root formation.

(a) The CI scores of each time point. The CI score of the S10 stage is higher than other developmental stages, which indicates the critical state or tipping point just before the transition for root swelling process.

(b) The expression levels of *IbNAC083* in storage roots (S18-S20) of WT and *IbNAC083*-RNAi

transgenic plants determined by RT-qPCR. Error bars indicates standard error (n = 9). * and ** indicate a significant difference compared to WT at $P < 0.05$ and < 0.01 , respectively, determined by Student's t -test.

(c) Phenotypes of field-grown wild type (WT) and *IbNAC083*-RNAi (*IbNAC083i*) transgenic sweet potato plants.

(d-f) Comparisons of root biomass (d), pencil root number (e), and storage root number (f). Root samples were collected from 9 independent plants per line. * and ** indicate a significant difference compared to WT at $P < 0.05$ and < 0.01 , respectively, determined by Student's t -test.

Figure 6. Dynamic network analysis of sweet potato root developmental transcriptome.

(a) Dynamics of *IbNAC083*-associated genes in terms of expression before and after the critical period. Expression of *IbNAC083* and its 63 neighbouring DEGs changes significantly (or inversed) from low (or high) at S8 stage to high (or low) at S12 stage (i.e., the expression of those genes inversed before and after the critical period, at S10 stage), implying key roles of DNB members in coordinating the critical transition of root swelling at S10 stage.

(b) Dynamic activity of the relative GO terms that involved *IbNAC083* and its neighbouring DEGs in different dynamic patterns.

(c) GO enrichment analysis of the DEGs in the initial swelling roots of *IbNAC083*-RNAi transgenic plants relative to the wild type (WT). The GO terms of biological processes with statistical significance (P -value ≤ 0.05) are shown. Three biological replicates were performed for each genotype.

(d) A heatmap illustrated the coexpression of *IbNAC083* and typical root development related genes. The 16 genes listed on the left of the broken line were also DEGs in the root developmental series transcriptomic data; 7 genes labelled by a green star had the coexpression relationships with *IbNAC083* by analysis of both the root developmental series transcriptomic expression profiling and the RNA-Seq data of WT and *IbNAC083*-RNAi transgenic plants. Genes in red showed positive coexpression with *IbNAC083* ($PCC > 0.8$), whereas genes in black showed negative coexpression with *IbNAC083* ($PCC < -0.8$).

(e) A molecular model of *IbNAC083* associated DNB network function in sweet potato initiation and

development.

Figure S1. Preferential/stage-specific expression of genes at different developmental stages of sweet potato roots.

(a) Heatmap showing the expression profile of preferentially expressed genes at different developmental stages. Color scale represents Z-score.

(b) Gene ontology (GO) enrichment of preferentially expressed genes at different developmental stages of sweet potato roots. The color scale at the bottom represents significance (corrected P -value).

Figure S2. Correlation between expression profiles of selected genes obtained from RNA-Seq and RT-qPCR analysis. Heatmaps represent expression profiles of selected genes (labelled on right side) obtained from RNA-Seq (left) and RT-qPCR (right) analysis. The color scale at the bottom represent Z-score. The values between the two heatmaps represent correlation value between the expression profiles obtained from RNA-Seq and RT-qPCR analysis for each gene. The correlation values above 0.70 are highlighted in bold.

Figure S3. Circos plots of developmental series expression profiles in comparison to previously published sweet potato root transcriptome data (Wang, Fang et al. 2015), as indicated underneath the plot.

Figure S4. Expression profile and subcellular localization of IbNAC083.

(a) Expression pattern of Arabidopsis *AtNAC083* gene on the UMAP plot from Zhang et al. (Zhang, Xu et al. 2019).

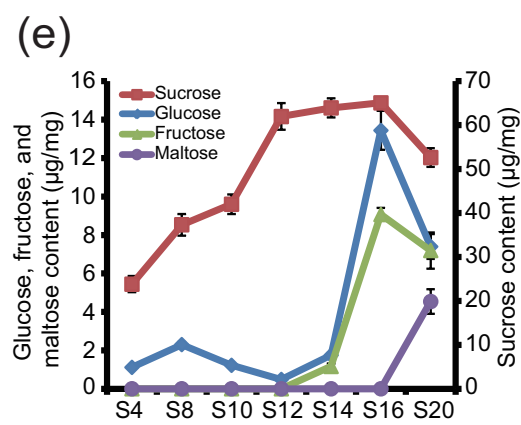
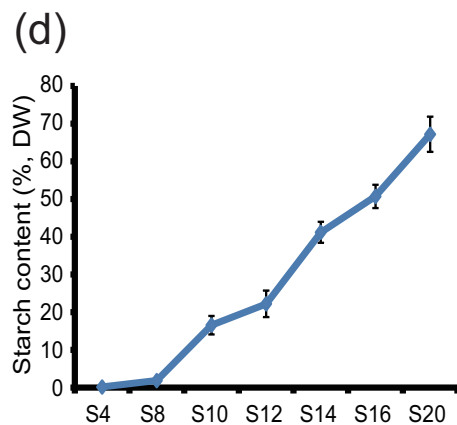
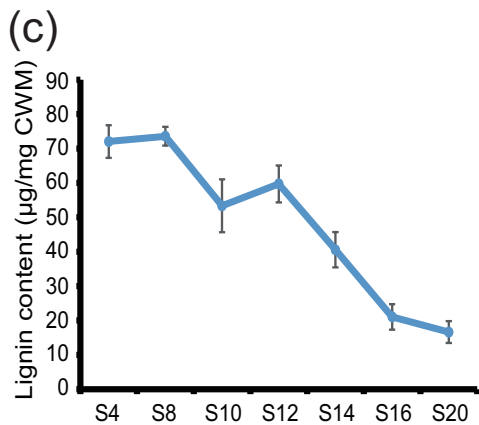
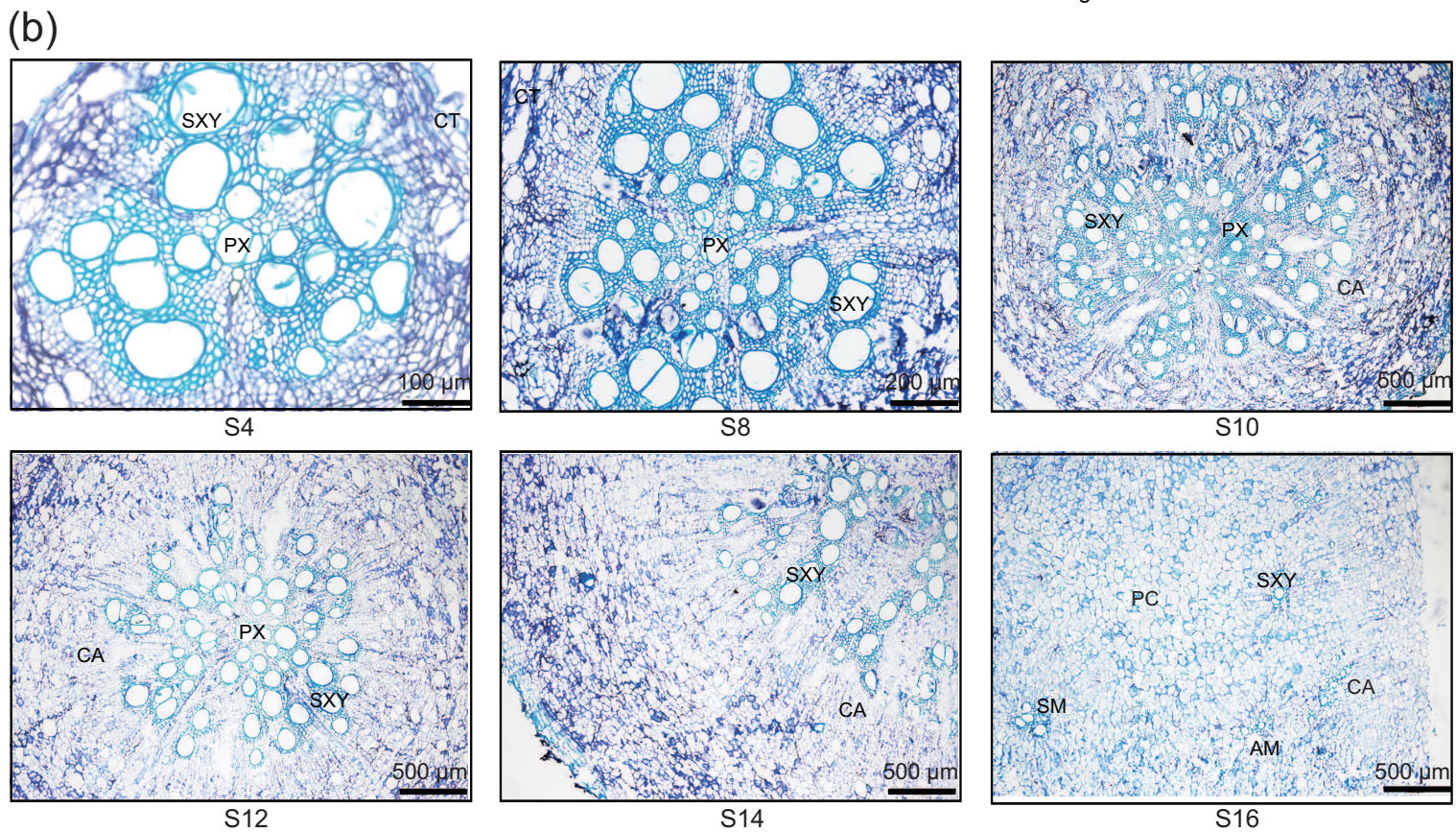
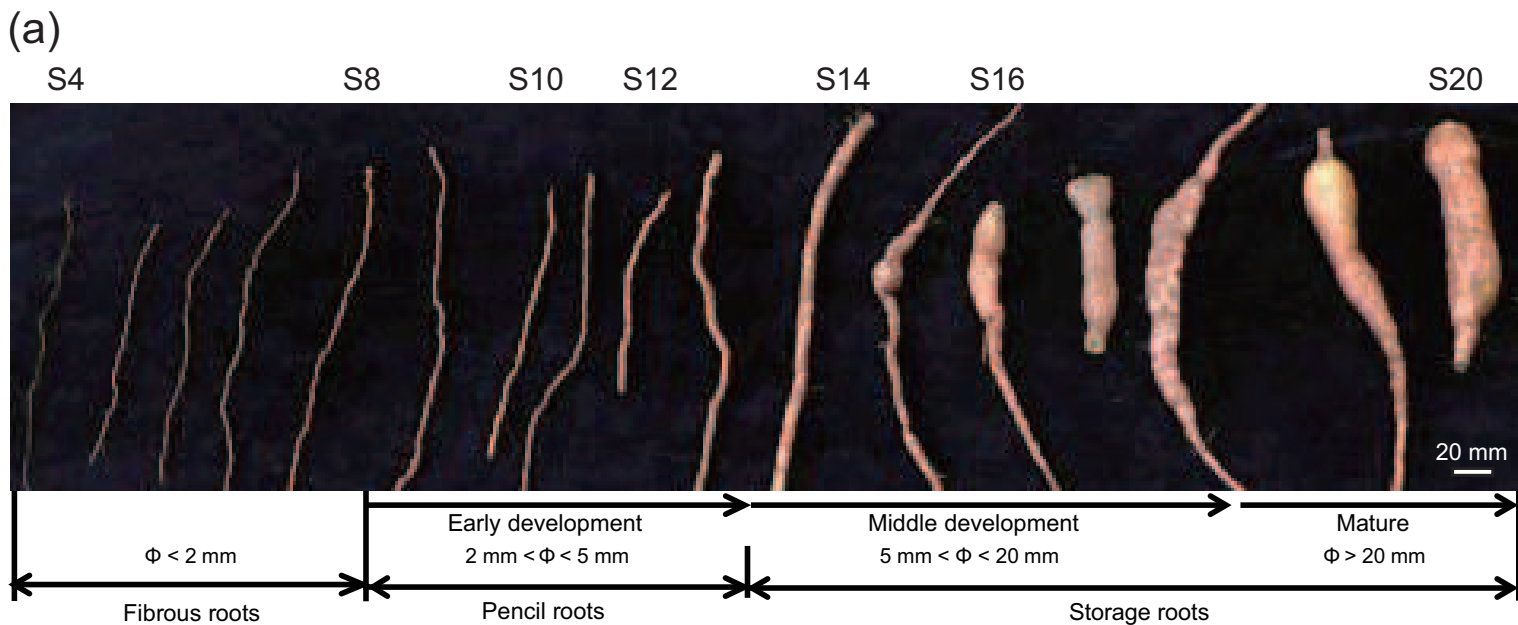
(b) GUS staining in root of *IbNAC083pro:uidA* transgenic Arabidopsis. The numbers in the lower left corner are the magnification fold.

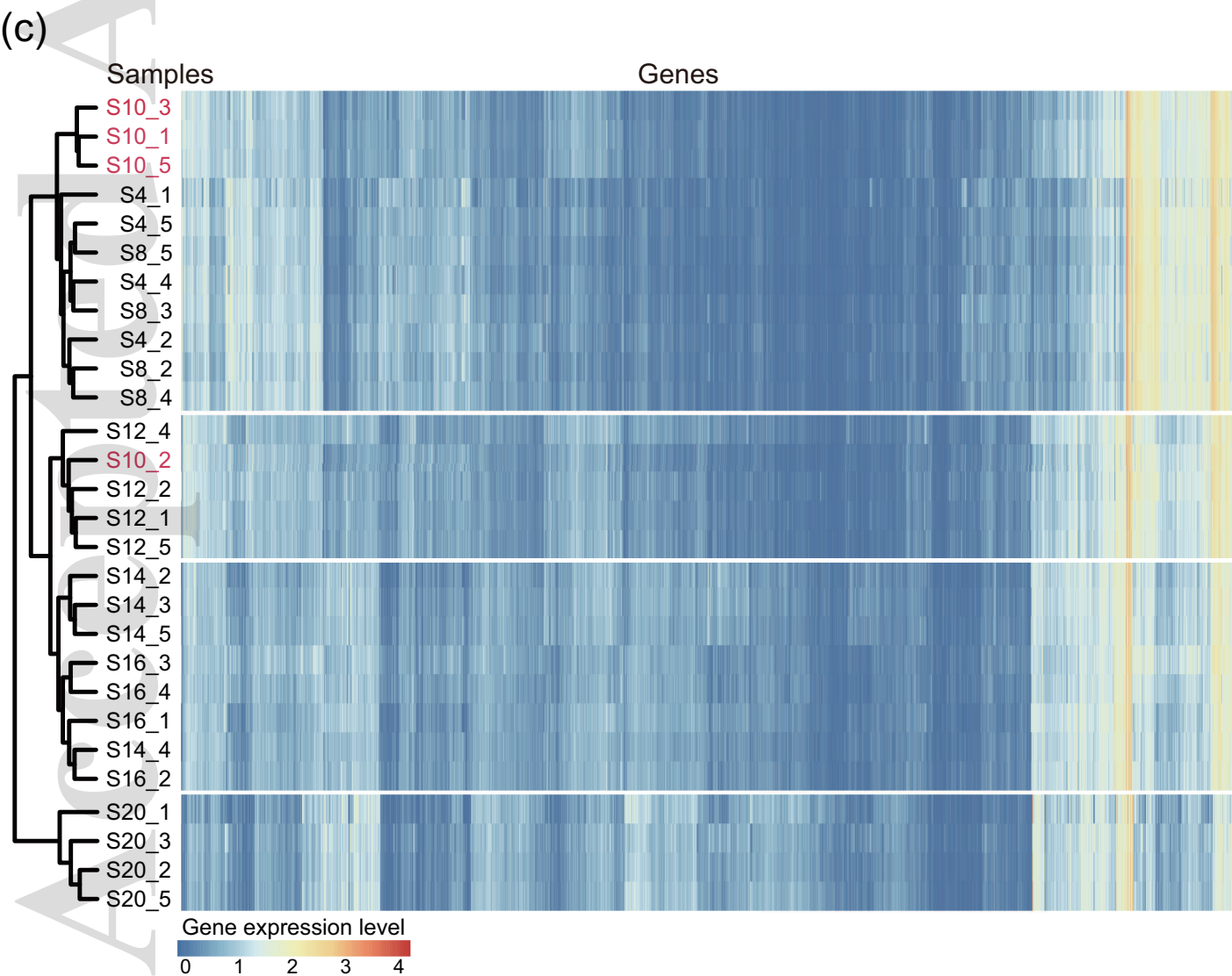
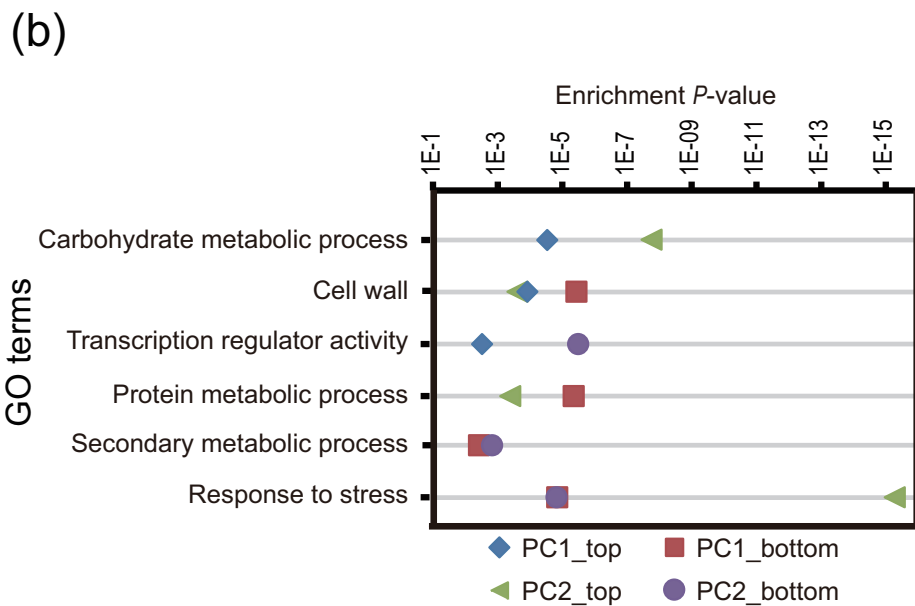
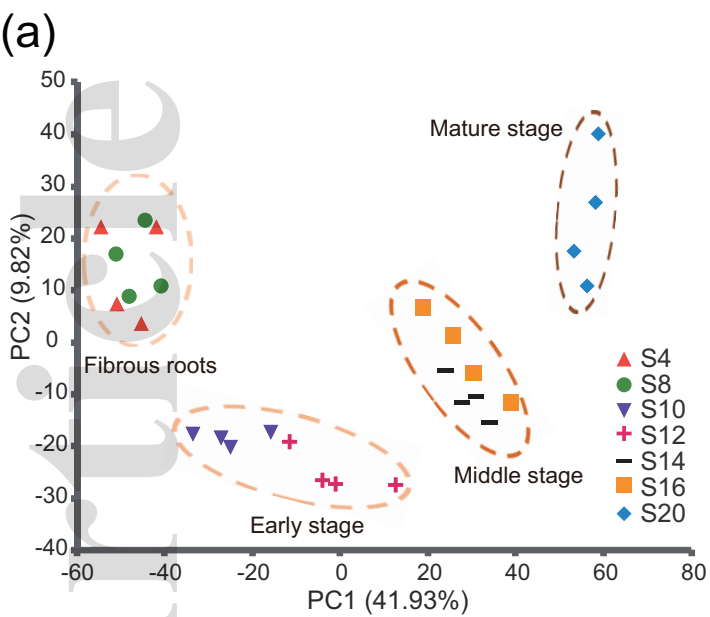
(c) Expression of *35S:IbNAC083-GFP* fusion protein in *Nicotiana benthamiana* leaf epidermal cells. 4',6-Diamidino-2-phenylindole (DAPI) was used to stain cell nuclei. *35S:GFP* protein was used as a negative control.

Figure S5. Changes in lignin and starch contents and related metabolic gene expression profiles in the initial swelling roots of WT (S12-S14) and *IbNAC083*-RNAi transgenic plants (S12-S14).

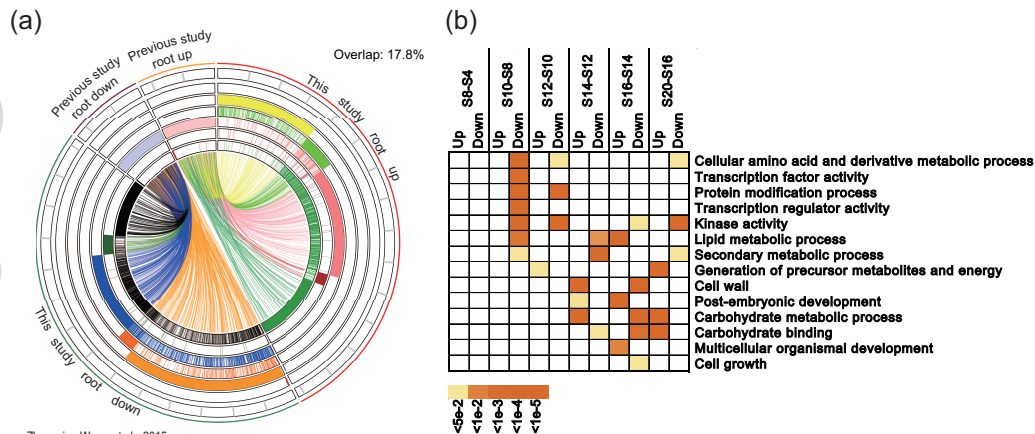
(a-b) Lignin content (a) and starch content (b) in the initial swelling roots of 5-month-old field-grown sweet potato plants. Error bars indicates standard error (n = 9). * and ** indicate a significant difference compared to WT at $P < 0.05$ and < 0.01 , respectively, determined by Student's *t*-test.

(c-d) RT-qPCR analysis of the changes in the transcript levels of major lignin biosynthetic genes (c) and starch metabolic genes (d) in the initial swelling roots of 5-month-old field-grown sweet potato plants. Lignin biosynthetic genes: *IbPAL*, phenylalanine lyase; *Ib4CL*, 4-coumarate-CoA ligase; *IbC4H*, cinnamic acid 4-hydroxylase; *IbCAD*, cinnamyl alcohol dehydrogenase; *IbCCR*, hydroxycinnamoyl-CoA reductase; *IbCOMT*, caffeic acid/5-hydroxyferulic acid *O*-methyltransferase; *IbCCoAOMT*, caffeoyl-CoA *O*-methyltransferase. Starch biosynthetic genes: *IbAGPa*, ADP-glucose pyrophosphorylase alpha subunit; *IbAGPb*, ADP-glucose pyrophosphorylase beta subunit; *IbGBSSI*, granule-bound starch synthase I; *IbSBEI*, starch branching enzyme I; *IbSBEII*, starch branching enzyme II; *IbSS*, soluble starch synthase. Genes involved in starch degradation: *Ib α -amylase* and *Ib β -amylase*. Error bars indicates standard error (n = 9). * and ** indicate a significant difference compared to WT at $P < 0.05$ and < 0.01 , respectively, determined by Student's *t*-test.

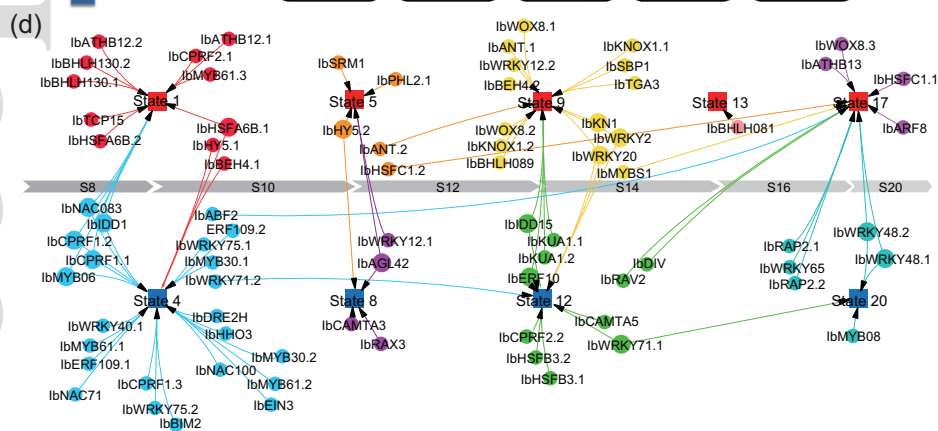
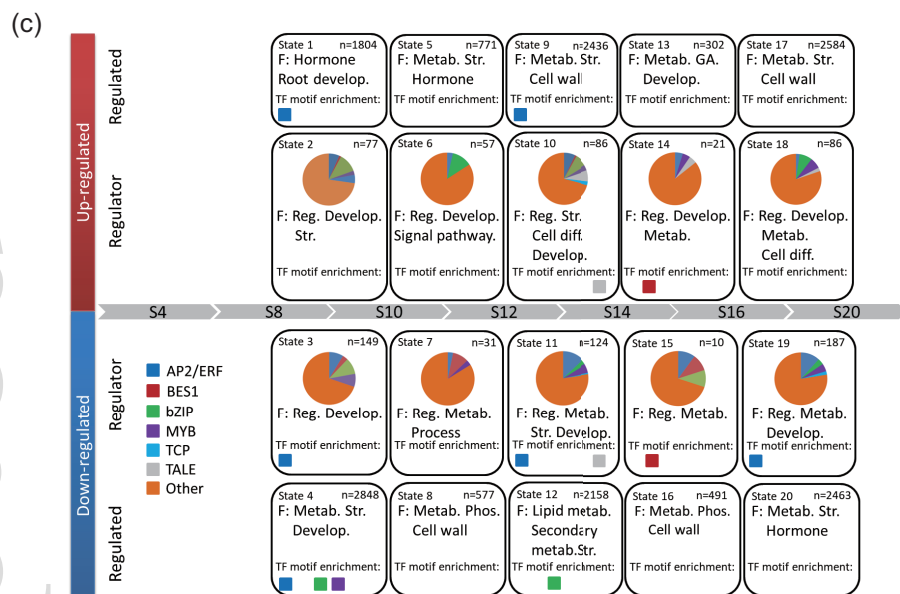




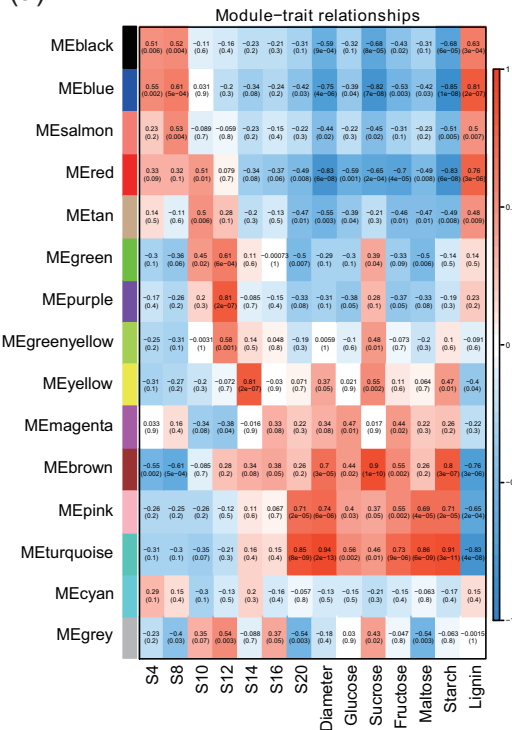
tpj_15478_f2.eps



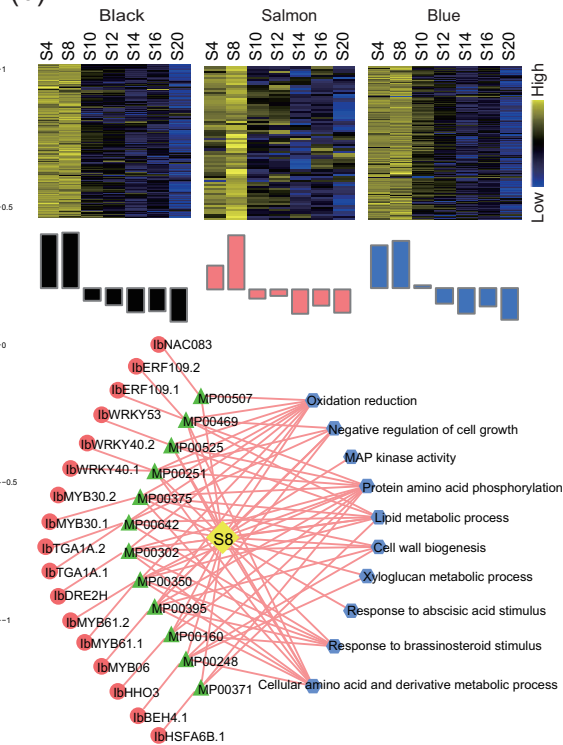
Zhangying Wang et al., 2015



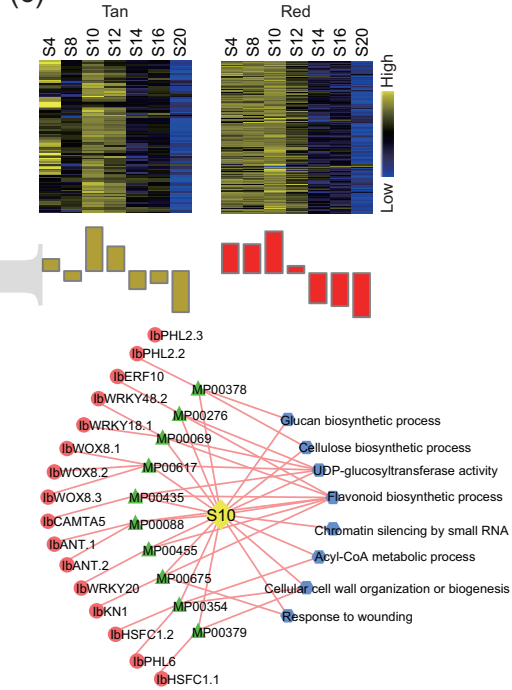
(a)



(b)



(c)



(d)

